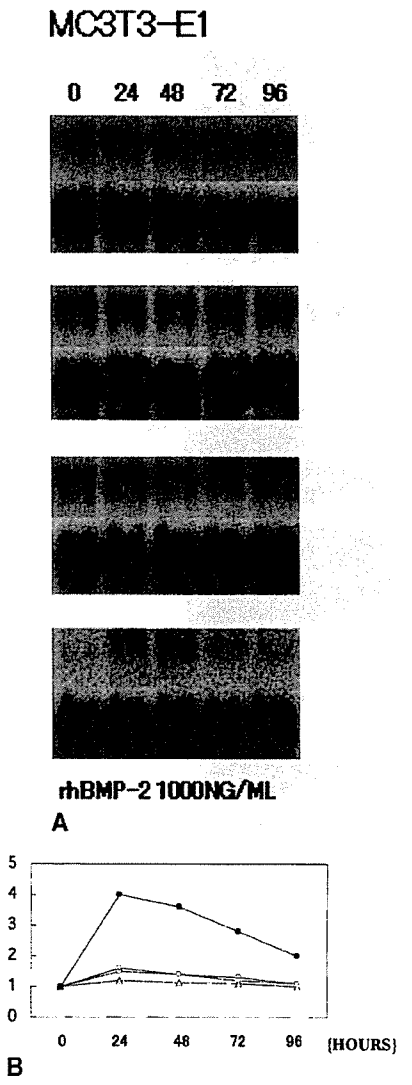

Fig. 5. Gene expression of BMPR-1A, -1B, -2, and Noggin for 0, 24, 48, 72, and 96 h after 1000 ng/ml rhBMP-2 stimulation in MC3T3-E1 cell line by Northern blot analysis (**A**) and quantitation of the data of Northern blot analysis by Densitometry (**B**). G3PDH mRNA levels (*the bottoms of all lanes* are G3PDH) obtained by Northern blotting were used for normalization (**A**). The score on hour 0 (just after BMP stimulation) was used as a standard (**B**). BMPR-1A and -2 were weakly induced after rhBMP-2 stimulation, peaked at 24 h, then decreased gradually. Noggin was also moderately induced after stimulation showed maximal expression at 24 h, then decreased thereafter. BMPR-1B was not induced during the course of the reaction

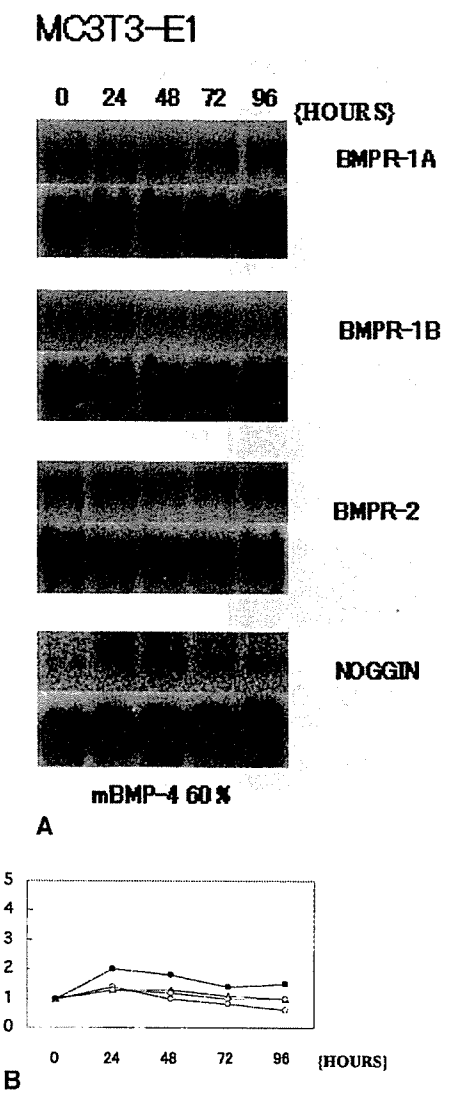

Fig. 6. Gene expression of BMPR-1A, -1B, -2, and Noggin for 0, 24, 48, 72, and 96 h after mBMP-4 (20%) stimulation in MC3T3-E1 cell line by Northern blot analysis (**A**) and quantitation of the data of Northern blot analysis by Densitometry (**B**). G3PDH mRNA levels (*the bottoms of all lanes* are G3PDH) obtained by Northern blotting were used for normalization (**A**). The score on hour 0 (just after BMP stimulation) was used as a standard (**B**). The gene expression pattern of the molecules after stimulation of mBMP-4 (20%) was similar to that seen after stimulation of 1000 ng/ml rhBMP-2, but the expression levels with mBMP-4 (20%) were smaller than those with 1000 ng/ml rhBMP-2

dependent manner suggests that BMP signaling in muscle tissue is regulated in a coordinated manner. OC is a well-characterized osteoblast differentiation marker, and MyoD is also a good marker for myoblastic differentiation [26]. Although the expression of MyoD was not detected in this study, the expression of OC was enhanced on day 2 after BMP-2 or -4 stimulation. These results indicate that BMP-induced osteogenic differentiation in muscle tissue might occur through a BMP/Smad signaling pathway, and muscle-derived primary culture cells might lose the muscle phenotype after BMP exposure.

The expression profiles were much more prominent for primary undifferentiated mesenchymal cells derived from muscle than for MC3T3-E1 or NIH3T3 cells in this study. Muscle-derived primary culture cells include a large population of undifferentiated mesenchymal cells, as described elsewhere [14]. Clearly, undifferentiated mesenchymal cells in muscle tissue are highly responsive to BMPs, based on

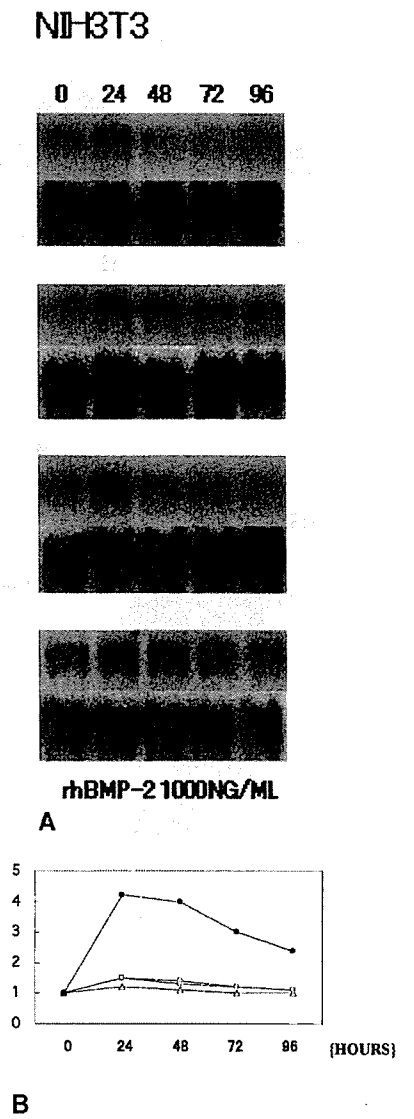

Fig. 7. Gene expression of BMPR-1A, -1B, -2, and Noggin for 0, 24, 48, 72, and 96 h after 1000 ng/ml rhBMP-2 stimulation in NIH3T3 cell line by Northern blot analysis (**A**) and quantitation of the data of Northern blot analysis by Densitometry (**B**). G3PDH mRNA levels (*the bottoms of all lanes* are G3PDH) obtained by Northern blotting were used for normalization (**A**). The score on hour 0 (just after BMP stimulation) was used as a standard (**B**). BMPR-1A and -2 were weakly induced after rhBMP-2 stimulation, peaked at 24 h, then decreased gradually. Noggin was moderately induced after stimulation showed maximal expression at 24 h, then decreased thereafter

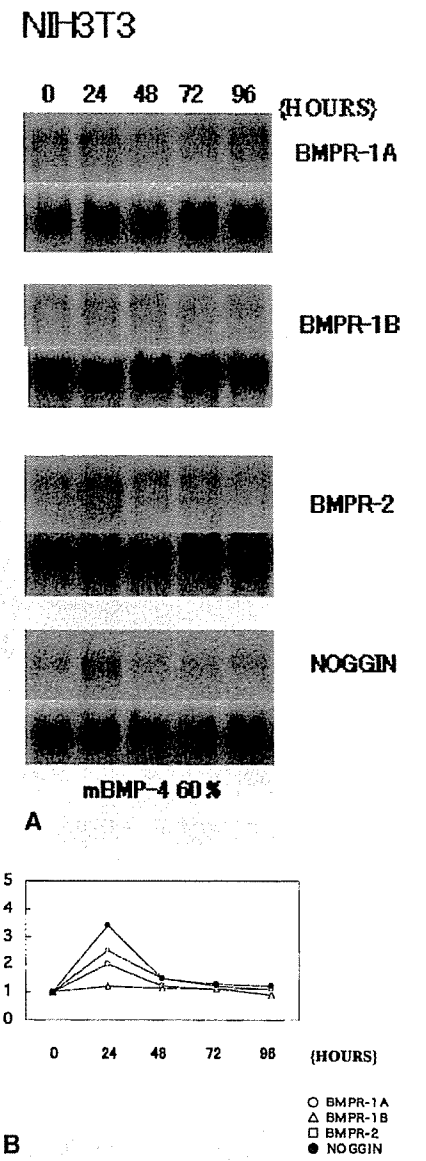

Fig. 8. Gene expression of BMPR-1A, -1B, -2, and Noggin for 0, 24, 48, 72, and 96 h after mBMP-4 (20%) stimulation in NIH3T3 cell line by Northern blot analysis (**A**) and quantitation of the data of Northern blot analysis by Densitometry (**B**). G3PDH mRNA levels (*the bottoms of all lanes* are G3PDH) obtained by Northern blotting were used for normalization (**A**). The score on hour 0 (just after BMP stimulation) was used as a standard (**B**). BMPR-1A and -2 were weakly induced after rhBMP-2 stimulation, peaked at 24 h, then decreased gradually. Noggin was moderately induced after stimulation showed maximal expression at 24 h, then decreased thereafter. BMPR-1B was not induced in all experimental stages. In NIH3T3 cells, the expression pattern was similar to that observed in the MC3T3-E1 culture experiments. Expression levels were greater in NIH3T3 cells than in MC3T3-E1 cells

the changes in gene and protein expression levels observed in this study. The proliferation and differentiation of osteoblasts from osteoprogenitor cells in murine bone marrow cultures induced by BMP-2 or -4 have been reported [27,28]. However, there have been few reports using muscle-derived primary culture cells with BMPs. In this study, the expression of BMP-related molecules was examined using undifferentiated mesenchymal cells derived from mouse muscle tissue.

The majority of undifferentiated mesenchymal cells in muscle-derived primary culture cells showed a fibroblastic appearance. These cells are considered to be heterogenous, and contain some kinds of precursor cells such as bone, cartilage, and muscle. They differentiate into each phenotype when they are placed in each differentiation condition.

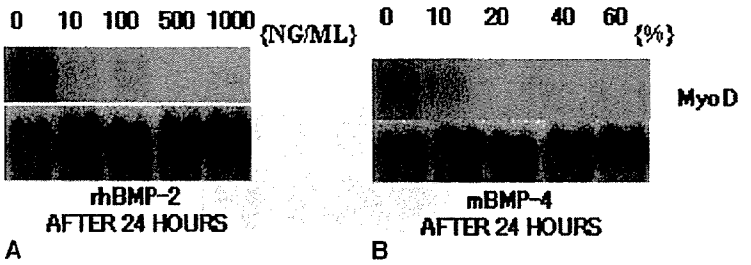

Fig. 9. The expression of MyoD in muscle-derived primary culture cells by Northern blot analyses. G3PDH mRNA levels obtained by Northern blotting were used for normalization. The expression of MyoD mRNA was not detected after BMP-2 or -4 exposure, and the expression was detected only at 0 and 24 h, and not after 24 h BMP stimulation

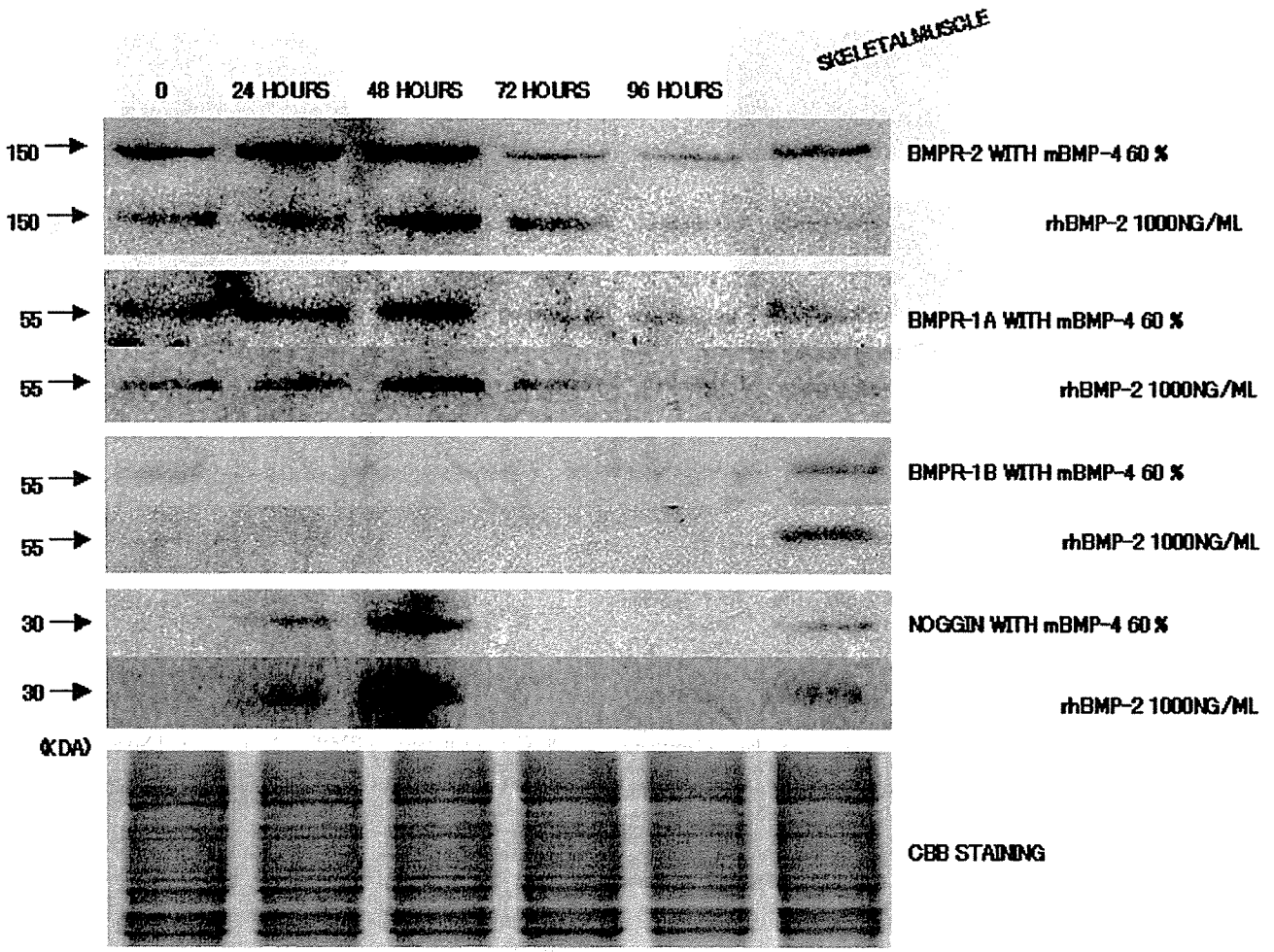

Fig. 10. Western blot analysis of BMPR-1A, -1B, -2, and Noggin after 60% mBMP-4 or 1000 ng/ml rhBMP-2 stimulation in muscle-derived primary culture cells. Equivalent loading and integrity of protein were confirmed by Coomassie brilliant blue staining on the gel (*lower panel*). Mouse skeletal muscle proteins were used as positive controls. BMPR-1A and -2 were detected at 0 h, induced at 24 h, peaked at 48 h, and then gradually decreased in both 60% mBMP-4 and 1000 ng/ml rhBMP-2 stimulation groups. Expression was greater for BMPR-2 than for BMPR-1A. BMPR-1B was not detectable during any stages in either treatment group. Noggin was not detected at 0 h, was up-regulated at 24 h, peaked at 48 h, and decreased thereafter

In our study, BMPs stimulated them to upregulate the expressions of a bone marker (OC) and cartilage markers (type II collagen and aggrecan, data not shown), but not the muscle marker examined previously. However, it is unclear whether bone and cartilage phenotypes were induced by BMPs in separate cells or in a single cell.

To further understand the potential autoregulatory mechanism in response to BMP, further gene expression

studies will be necessary. Ultimately, this knowledge may provide new approaches to the regulation of local and systemic bone formation.

References

1. Aspenberg P, Turek T (1996) BMP-2 for intramuscular bone induction: effect in squirrel monkeys is dependent on implantation site. Acta Orthop Scand 67:3–6
2. Itoh H, Ebara S, Kamimura M, Tateiwa Y, Kinoshita T, Yuzawa Y, Takaoka K (1999) Experimental spinal fusion with use of recombinant human bone morphogenetic protein. 2. Spine 24:1402–405
3. Takaoka K, Yoshikawa H, Hashimoto J, Ono K, Matsui M, Nakazato H (1994) Transfilter bone induction by Chinese hamster ovary (CHO) cells transfected by DNA encoding bone morphogenetic protein-4. Clin Orthop 300:269–273
4. Kaplan FS, Shore EM (1999) Illustrative disorders of ectopic skeletal morphogenesis: a childhood parallax for studies in gravitational and space biology. Gravit Space Biol Bull 12:27–38
5. Miyazono K, Ichijo H, Heldin CH (1993) Transforming growth factor-beta: latent forms, binding proteins and receptors. Growth Factors 8:11–22
6. Fujii M, Takeda K, Imamura T, Aoki H, Sampath TK, et al. (1999) Roles of bone morphogenetic protein type I receptors and Smad proteins in osteoblast and chondroblast differentiation. Mol Biol Cell 10:3801–3813
7. Ishidou Y, Kitajima I, Obama H, Maruyama I, Murata F, et al. (1995) Enhanced expression of type I receptors for bone morphogenetic proteins during bone formation. J Bone Miner Res 10: 1651–1659
8. Onishi T, Ishidou Y, Nagamine T, Yone K, Iamamura T, et al. (1998) Distinct and overlapping patterns of localization of bone morphogenetic protein (BMP) family members and a BMP type II receptor during fracture healing in rats. Bone 22:605–612
9. Kaneko H, Arakawa T, Mano H, Kaneda T, Ogasawara A, et al. (2000) Direct stimulation of osteoclastic bone resorption by bone morphogenetic protein (BMP)-2 and expression of BMP receptors in mature osteoclasts. Bone 27:479–486
10. Nakamura Y, Wakitani S, Nakayama J, Wakabayashi S, Horiuchi H, Takaoka K (2003) Temporal and spatial expression profiles of BMP receptors and Noggin during BMP-2-induced ectopic bone formation. J Bone Miner Res 18:1854–1862
11. Horiuchi H, Saito N, Kinoshita T, Wakabayashi S, Tsutsumimoto T, Takaoka K (2001) Enhancement of bone morphogenetic protein-2-induced new bone formation in mice by the phosphodiesterase inhibitor pentoxifylline. Bone 28:290–294
12. Takaoka K, Yoshikawa H, Hashimoto J, Ono K, Matsui M, Nakazato H (1994) Transfilter bone induction by Chinese hamster ovary (CHO) cells transfected by DNA encoding bone morphogenetic protein-4. Clin Orthop 300:269–273
13. Tsutsumimoto T, Wakabayashi S, Kinoshita T, Horiuchi H, Takaoka K (2002) A phosphodiesterase inhibitor, pentoxifylline, enhances the bone morphogenetic protein-4 (BMP-4)-dependent differentiation of osteoprogenitor cells. Bone 31:396–401
14. Yaffe D (1973) Rat skeletal muscle cells. In: Kruse PF, Patterson MK (eds) Tissue Culture, vol 16. Academic Press, New York, p 106–114
15. Yoshimura Y, Nomura S, Kawasaki S, Tsutsumimoto T, Shimizu T, Takaoka K (2001) Colocalization of Noggin and bone morphogenetic protein-4 during fracture healing. J Bone Miner Res 16:876–884
16. Kamiya N, Jikko A, Kimata K, Damsky C, Shimizu K, Watanabe H (2002) Establishment of a novel chondrocytic cell line N1511 derived from p53-null mice. J Bone Miner Res 17:1832–1842
17. Jiao K, Zhou Y, Hogan BL (2002) Identification of mZnf8, a mouse Kruppel-like transcriptional repressor, as a novel nuclear interaction partner of Smad1. Mol Cell Biol 22:7633–7644
18. Yamaguchi A, Ishizuya T, Kitou N, Wada Y, Katagiri T, et al. (1996) Effects of BMP-2, BMP-4, and BMP-6 on osteoblastic differentiation of bone marrow-derived stromal cell lines, ST2 and MC3T3-G2/PA6. Biochem Biophys Res Commun 220:366–371
19. Zhao M, Harris SE, Horn D, Geng Z, Nishimura R, Mundy GR, Chen D (2002) Bone morphogenetic protein receptor signaling is necessary for normal murine postnatal bone formation. J Cell Biol 157:1049–1060
20. Wlodarski KH, Reddi AH (1986) Importance of skeletal muscle environment for ectopic bone induction in mice. Folia Biol (Krakow) 34:425–434
21. Chen D, Ji X, Harris MA, Feng JQ, Karsenty G, et al. (1998) Differential roles for bone morphogenetic protein (BMP) receptor type 1B and 1A in differentiation and specification of mesenchymal precursor cells to osteoblast and adipocyte lineages. J Cell Biol 142:295–305
22. Akiyama S, Katagiri T, Namiki M, Yamaji N, Yamamoto N, et al. (1997) Constitutively active BMP type I receptors transduce BMP-2 signals without the ligand in C2C12 myoblasts. Exp Cell Res 235:362–369
23. Gazzerro E, Gangji V, Canalis E (1998) Bone morphogenetic proteins induce the expression of Noggin, which limits their activity in cultured rat osteoblasts. J Clin Invest 15:2106–2114
24. Nifuji A, Noda M (1999) Coordinated expression of Noggin and bone morphogenetic proteins (BMPs) during early skeletogenesis and induction of Noggin expression by BMP-7. J Bone Miner Res 14:2057–2066
25. Attisano L, Tuen Lee-Hoeflich S (2001) The Smads Genome. Biol 2:Reviews3010
26. Yamamoto N, Akiyama S, Katagiri T, Namiki M, Kurosawa T, Suda T (1997) Smad1 and smad5 act downstream of intracellular signalings of BMP-2 that inhibits myogenic differentiation and induces osteoblast differentiation in C2C12 myoblasts. Biochem Biophys Res Commun 238:574–580
27. Zou H, Wieser R, Massague J, Niswander L (1997) Distinct roles of type I bone morphogenetic protein receptors in the formation and differentiation of cartilage. Genes Dev 11:2191–2203
28. Abe E, Yamamoto M, Taguchi Y, Lecka-Czernik B, O'Brien CA, et al. (2000) Essential requirement of BMPs-2/4 for both osteoblast and osteoclast formation in murine bone marrow cultures from adult mice: antagonism by Noggin. J Bone Miner Res 15:663–673

Available online at www.sciencedirect.com
SCIENCE DIRECT
Journal of Clinical Neuroscience 13 (2006) 250–256
Journal of Clinical Neuroscience
www.elsevier.com/locate/jocn

Laboratory study

Coordinate expression of BMP-2, BMP receptors and Noggin in normal mouse spine

Yukio Nakamura, Hiroyuki Nakaya, Naoto Saito, Shigeyuki Wakitani *

Department of Orthopaedic Surgery, Shinshu University School of Medicine, Asahi 3-1-1, Matsumoto, 390-8621, Japan

Received 25 August 2004; accepted 31 May 2005

Abstract

The purpose of this study was to determine the localization of bone morphogenetic protein-2 (BMP-2), BMP receptors (BMPRs) and Noggin in mouse spinal tissues. The coordinate expression of these positive and negative regulators of BMP signaling may elucidate regulatory mechanisms for bone induction in the spine. Whole spines from 3-week-old mice were used and the spatial expression profiles of BMP-2, BMPR-1a, -1b, -2 and Noggin were examined using in situ hybridization. BMP-2, BMPR-1b and -2 were observed in bone marrow cells in the vertebrae, chondrocytes, hyaline cartilage cells and fibrous cells in the intervertebral discs and neurons of the spinal cord in the entire spine. BMPR-1a was also observed in these cells, but only in the cervical spine. Noggin was expressed in bone marrow cells in the vertebrae, chondrocytes and hyaline cartilage cells and fibrous cells in the intervertebral discs in the entire spine and in neurons in the spinal cord in the cervical and thoracic regions. Noggin was also expressed in the anterior longitudinal, posterior longitudinal and yellow ligaments in the cervical spine, and in the fibrous cells in the anterior longitudinal and yellow ligaments of the lumbar spine.

Keywords: BMP-related molecules; In situ hybridization; Localization; Spine

1. Introduction

Signaling by BMPs requires binding of the BMP molecules (BMP-2, -4 and -7) to one of two types of serine-threonine BMP receptors (BMPRs), known as type 1 (1a and 1b) and type 2 BMPR.[1] These receptors then phosphorylate intra-cellular proteins, including the Smads (Smad 1–5) to effect intracellular signaling and physiological responses.[2–5] Therefore, BMPR expression is a prerequisite for biological action of BMP. An important growth factor related to BMP and BMPR is Noggin, a molecule that has been shown to antagonize the action of the BMPs.[6–9] The coordinate expression of these positive and negative regulators of BMP signaling points to a potential regulatory mechanism for bone induction.

BMPs are involved in the morphogenesis and development of many organ systems. The expression of BMPR-1a or -1b has been reported during bone formation in fracture repair and pathological ectopic bone formation in spinal ligaments.[3,5,10] BMPs also play a key role in the development and growth of neurons, bone and cartilage, therefore, they may be important in the morphogenesis of spinal systems. There is also evidence from animal models that BMPs play a role in diseases characterised by mineralization of ligaments, including ossification of the anterior or posterior longitudinal ligament, ankylosing spondylitis, ossification of the ligamentum flavum and spinal spondylosis. However, there have been no reports published to date that show the distribution of BMP-2, BMPR or Noggin in normal animal models using whole spinal tissue.[11–13] Although previous reports have described aspects of spinal ossification, little is known about the molecular mechanisms that drive this event in spinal tissue.

Therefore, we used in situ hybridization to define the spatial expression profiles and localization of BMP-2, BMPRs, and Noggin in the whole spine of normal mice.

* Corresponding author. Tel.: +81 263 37 2659; fax: +81 263 35 8844.
E-mail address: wakitani@hsp.md.shinshu-u.ac.jp (S. Wakitani).

0967-5868/$ - see front matter © 2006 Elsevier Ltd. All rights reserved.
doi:10.1016/j.jocn.2005.05.011

2. Materials and methods

2.1. Histological preparation

Three-week-old male ddY mice were used, purchased from Nippon SLC Co. (Shizuoka, Japan) and housed in cages with free access to food and water for 1 week prior to sacrifice. Mice were sacrificed with diethyl ether.

Specimens were removed en bloc and fixed in 10% neutral buffered formalin. They were decalcified with 20% EDTA after washing with 0.1 mol/L phosphate-buffered saline (PBS). They were then dehydrated through graded ethanol, and embedded in paraffin. Sections of 4-μm thickness were prepared using a microtome, and processed for hematoxylin and eosin (*H/E*) staining.

2.2. RNA probes for in situ hybridization

A 0.50-kilobase (kb) fragment of mouse BMPR-1a cDNA, a 0.47-kb fragment of mouse BMPR-1b cDNA, a 0.55-kb fragment of mouse BMPR-2 cDNA, and a 0.32-kb fragment of mouse Noggin cDNA were used as templates to synthesize RNA probes. They were subcloned into pBluescript SK (+) plasmid (Stratagene, La Jolla, CA). The BMP-2 and Noggin cDNAs were obtained by reverse transcription polymerase chain reaction (RT-PCR), and the Noggin primers for PCR were as described previously.[14] The BMPR primers for PCR were as follows: BMPR-1a: 5′-CTCATGTTCAAGGGCAG-3′ (5′ sense) and 5′-CCCCTGCTTGAGATACTC-3′ (3′ antisense; 346–362 and 850-833, respectively). BMPR-1b: 5′-ATGTGGGCACCAAGAAG-3′ and 5′-CTGCTCC-AGCCCAATGCT-3′ (215-231 and 681-664, respectively). BMPR-2: 5′- GTGCCCTGGCTGCTATGG-3′ and 5′-TGCCGCCTCCATCATGTT-3′ (47-64 and 592-575, respectively). Nucleotide sequences of the cDNA fragments were checked and found to be identical to mouse BMPRs (BMPR-1a: NM009758, BMPR-1b: NM007560, BMPR-2: NM007561).

For in situ hybridization, each plasmid containing a BMP-2 or Noggin cDNA fragment was linearized as described previously.[14] Plasmids with BMPR cDNA fragments were either linearised with *Xba I* and transcribed with T3 RNA polymerase to generate long antisense RNA probes or linearised with *Xho I*, and transcribed with T7 RNA polymerase to generate sense RNA probes.

2.3. In situ hybridization

In situ hybridization was carried out as described previously.[14,15] Mice were sacrificed and fixed by vascular perfusion with 4% paraformaldehyde (PFA). Tissue specimens were then removed, and fixed in fresh PFA solution for 24 hours. After fixation, the tissues were embedded in paraffin, and 7-μm sections were cut and then mounted on sialinized, APS-coated slides. They were stored at 4 °C until use. Sections were blow-dried, deparaffinized, rehydrated, and fixed with 4% PFA for 10 min at room temperature. They were then treated with PBS for 5 min, Proteinase K (15 μg/mL) in PBS for 10 min at 37 °C, 4% PFA for 10 min, 0.2N HCl for 10 min, 0.1 mol triethanolamine for 5 min and 1% acetic acid 0.1 mol triethanolamine for 10 min at room temperature. The hybridization solution contained 50% deionized formamide, 5x SSC, 1% SDS, 50 μ/mL heparin and approximately 75 ng/slide of RNA probe. Digoxigenin (DIG)-labeled single-strand antisense RNA probes for BMP-2, BMPR-1a, -1b, -2 and Noggin prepared with a DIG-labeling Mix (x10 concentration) were hybridized with the histological sections, covered with siliconized coverglasses, and incubated at 60 °C for 16 hours in a humid chamber. After hybridization, the slides were washed for 10 min twice with 2x SSC at 50 °C, and 0.2x SSC at 50 °C. Hybridised DIG-labelled probes were detected using Tris buffered saline (TBS) (0.3% Tween 20), blocking solution, anti DIG-alkaline phosphatase-labelled antibody (1:2000), TBS (0.3% Tween 20) twice, APB buffer (0.1 M Tris-HCl (Ph 9.5), 0.1 M NaCl, 50 mM $MgCl_2$), and then developed with NBT/BCIP substrate. Thereafter, the slides were mounted with Kernechtrot stain solution (Muto Chemical Co., Tokyo, Japan).

The controls consisted of hybridization with the sense probes and omission of either the antisense RNA probe or the anti-DIG antibody.

This study was carried out in accordance with the World Medical Association Declaration of Helsinki.

3. Results

3.1. Expression of BMP-2

BMP-2 was moderately and broadly detected in bone marrow cells in vertebral bone in the cervical, thoracic and lumbar spine. It was weakly detected in chondrocytes, hyaline cartilage cells and fibrous cells in the intervertebral discs in the cervical, thoracic, and lumbar spine. This pattern of moderate staining was repeated in the neurons of the spinal cord and it was also weakly detected in fibrous cells in parts of the yellow ligament in the cervical, thoracic and lumbar spine (Fig. 1A, B).

3.2. Expression of BMPR-1a

In the cervical spine, BMPR-1a was stained lightly and diffusely in bone marrow cells in vertebral bone, but not in the intervertebral discs. A moderate and more focused pattern of staining was observed in the neurons in the spinal cord. BMPR-1a was stained in the fibrous cells in the yellow ligament, but not in the anterior or posterior longitudinal ligaments. No staining for BMPR-1a was observed in any part of the thoracic or lumbar spine or the surrounding tissues (data not shown).

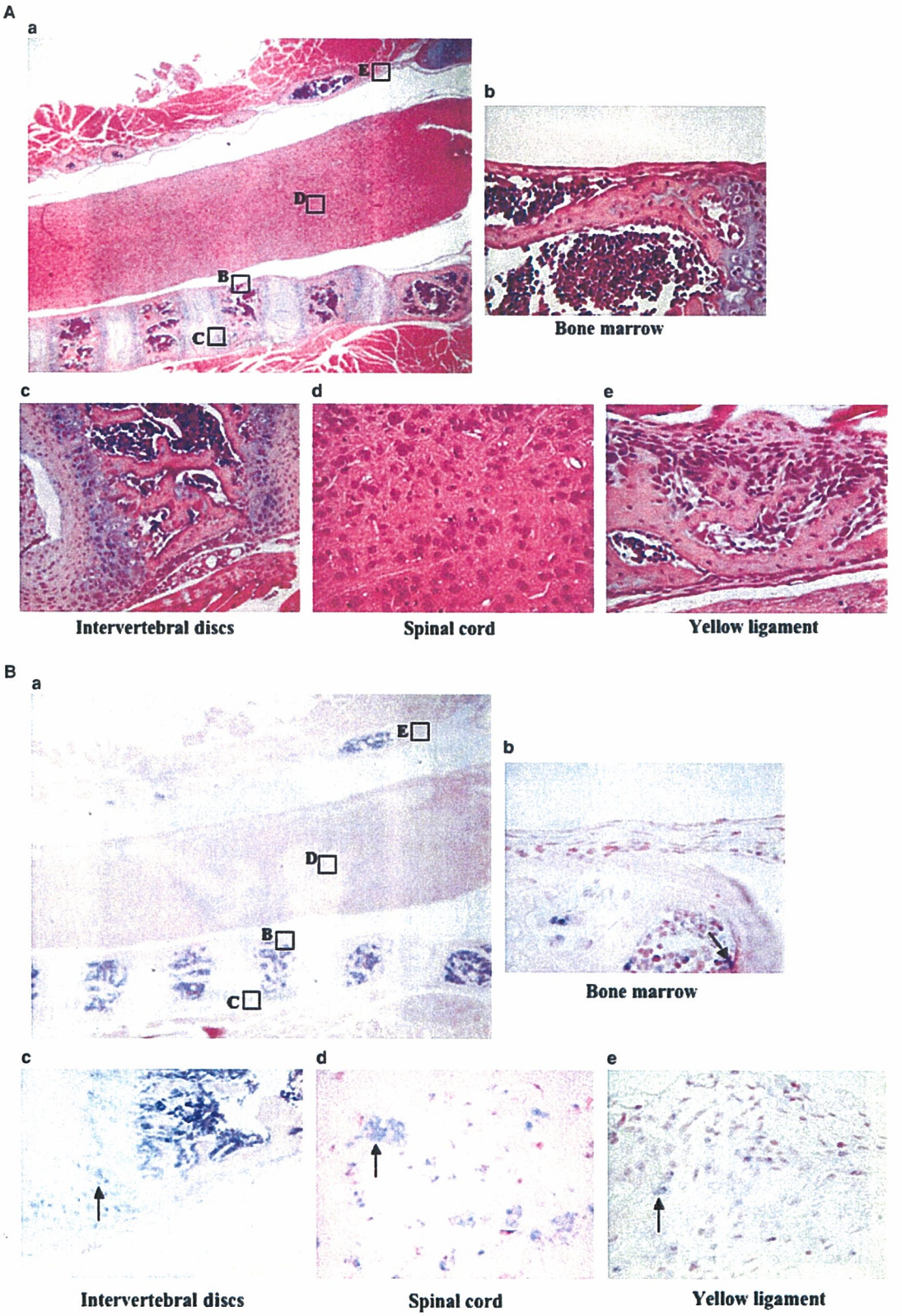

Fig. 1A. (a) Hematoxylin and eosin histochemistry of the cervical spine of the 3-week-old mouse corresponding to in situ hybridization of BMP-2 in Fig. 1B. (b) In situ hybridization of BMP-2 in the cervical spine of the 3-week-old mouse. In the whole cervical spine (a: original magnification: ×16), vertebral bone (b: original magnification: ×400), intervertebral discs (c: original magnification: ×400), spinal cord (d: original magnification: ×400) and yellow ligament (e: original magnification: ×400). Arrow in (b) indicates moderate expression in bone marrow cells and arrows in (c) indicate weak expression in hyaline cartilage cells. Arrow in (d) indicates moderate expression in neurons and arrows in (e) indicate weak staining of fibrous cells.

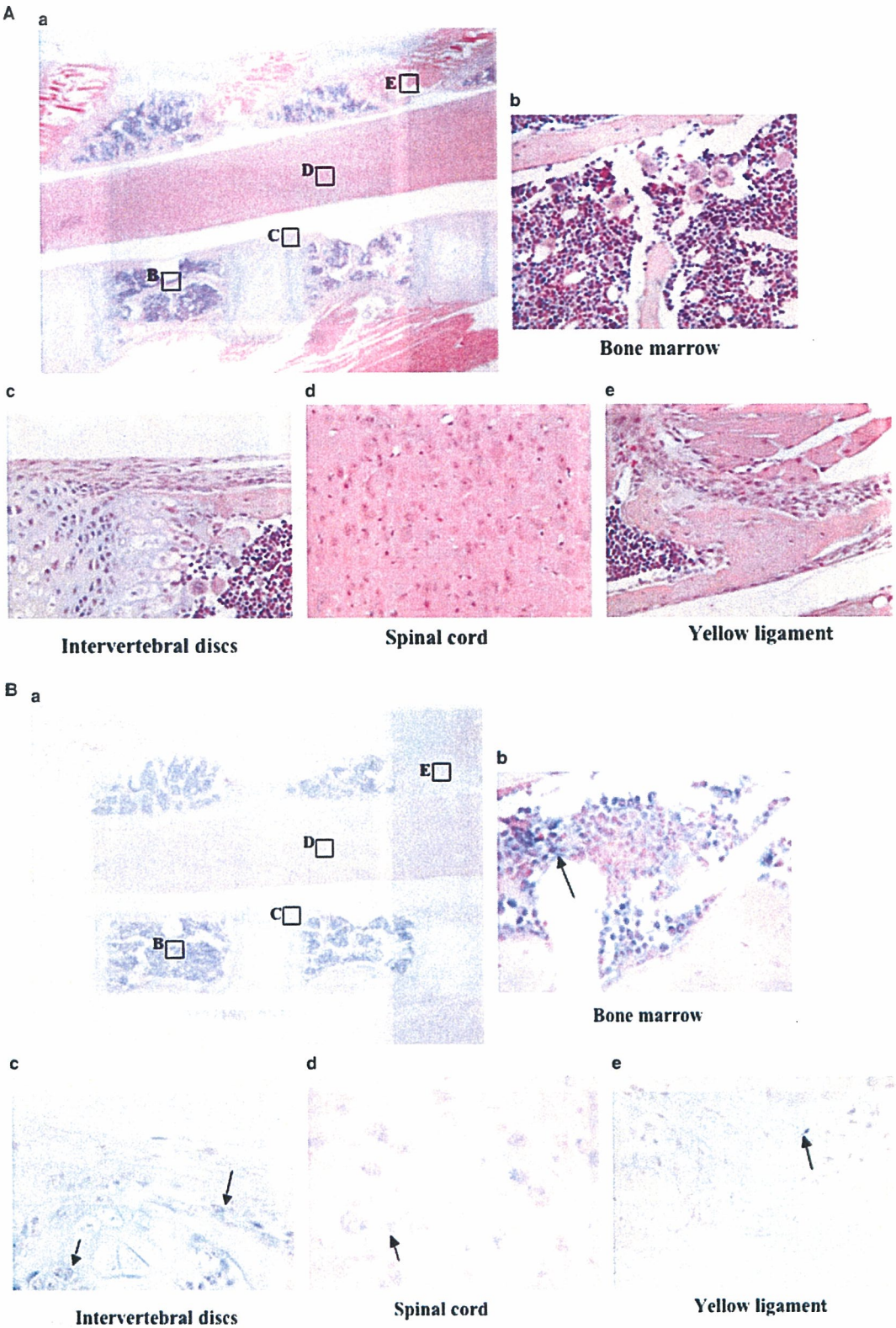

Fig. 2A. (a) Hematoxylin and eosin histochemistry of the lumbar spine of the 3-week-old mouse corresponding to in situ hybridization of BMPR-1b in Fig. 2B. (b) In situ hybridization of BMPR-1b in the lumbar spine of the 3-week-old mouse. In the whole lumbar spine (a: original magnification: ×16), vertebral bone (b: original magnification: ×400), intervertebral discs (c: original magnification: ×400), spinal cord (d: original magnification: ×400) and yellow ligament (e: original magnification: ×400). Arrow in (b) indicates strong expression in bone marrow cells and arrows in (c) indicate moderate expression in osteoblastic cells, multinuclear chondrocytes and hyaline cartilage cells. Arrow in (d) indicates moderate expression in neurons and arrows in (e) indicate weak staining of fibrous cells.

3.3. Expression of BMPR-1b

BMPR-1b was strongly and broadly detected in bone marrow cells, diffusely in osteoblastic cells and multinuclear cells in the vertebral bone of the cervical, thoracic and lumbar spine. It was also moderately stained in chondrocytes, hyaline cartilage cells, and fibrous cells in the intervertebral discs in the cervical, thoracic and lumbar spine. This pattern of staining was repeated in the neurons of the spinal cord in the cervical, thoracic and lumbar spine. It was also stained in fibrous cells in parts of the yellow ligament, but only in the lumbar spine (Fig. 2A, B).

3.4. Expression of BMPR-2

In the whole spine, BMPR-2 was stained lightly and diffusely in bone marrow cells in vertebral bone and in chondrocytes, hyaline cartilage cells and fibrous cells in the intervertebral discs. Moderate staining was observed in neurons in the spinal cord, however BMPR-2 was not observed in the ligaments (data not shown).

3.5. Expression of Noggin

Noggin was strongly and broadly detected in bone marrow cells in vertebral bone, moderately in chondrocytes, hyaline cartilage cells and fibrous cells in intervertebral discs, the neurons in the spinal cord in cervical spine and only weakly in parts of the anterior longitudinal, posterior longitudinal and yellow ligaments. It was also stained weakly in bone marrow cells in vertebral bone, chondrocytes, hyaline cartilage cells and fibrous cells in the intervertebral discs and moderately in neurons of the spinal cord in the thoracic spine. It was stained in bone marrow cells in vertebral bone, chondrocytes, hyaline cartilage cells and fibrous cells in intervertebral discs, and in the fibrous cells in parts of the anterior longitudinal and yellow ligaments in the lumbar spine (Fig. 3A, B).

4. Discussion

The expression and distribution of BMP-2, BMPR-1b and -2 was confined to bone marrow cells in vertebral bone, chondrocytes, hyaline cartilage cells and fibrous cells in the intervertebral discs and neurons of the spinal cord in the entire spine. BMPR-1a was expressed similarly in those cells, but only very weakly in the cervical spine. These results suggest the coordinate expression of BMP-2, BMPR-1b and -2 might be associated with the development of the spine. BMPR-1a and -1b share approximately 85% amino acid sequence identity,[2] but each receptor has a different function. BMPR-1a and -2 are expressed ubiquitously in various tissues, and are essential for proper regulation of the later stage of chondrocyte differentiation. BMPR-1b is observed mainly in the brain in animal models, and is necessary for the early stages of mesenchymal condensation and cartilage formation. This receptor is also involved in BMP-mediated programmed cell death.[1,2] In addition, co-expression of BMPR-2 with BMPR-1a or -1b increases binding affinity, and dramatically enhances biological activity.[3]

Noggin is a specific antagonist of BMPs, and blocks the binding of BMP to the BMPRs and thus, the subsequent actions of this protein.[14] In our study, Noggin was strongly expressed in bone marrow cells in vertebral bone, with a more moderate level in chondrocytes, hyaline cartilage cells and fibrous cells in intervertebral discs and in the neurons in the spinal cord of the cervical spine. In the thoracic spine, Noggin was also observed weakly in bone marrow cells in vertebral bone and chondrocytes, hyaline cartilage cells and fibrous cells in the intervertebral discs. A similar pattern of staining was also noted in the lumbar spine. There have been no published reports regarding the localization of Noggin in mice spinal tissues to date. The expression of Noggin in normal spinal tissues documented in this study points to the possibility of a negative feedback mechanism for BMP stimulation.

In ligaments, BMPR-1a was stained in the fibrous cells in the yellow ligament of the cervical spine, BMP-2 in the fibrous cells in the yellow ligament of the entire spine, BMPR-1b in the fibrous cells in the yellow ligament of the lumbar spine and BMPR-2 expression was not observed. Noggin was expressed weakly in parts of the anterior longitudinal, posterior longitudinal and yellow ligaments in the cervical spine and also in the fibrous cells in parts of the anterior longitudinal and yellow ligaments in the lumbar spine. In summary, these results indicate that the expression of BMP-2 in the whole spine, BMPR-1a and Noggin in the cervical spine, BMPR-1b and Noggin in lumbar spine might have a relationship with the ossification of ligaments.

The central nervous system is organized mainly by neurons, astrocytes and oligodendrocytes. Neurons form a large network with axons, astrocytes and oligodendrocytes. Astrocyte differentiation is induced synergistically by BMP-2 and leukemia inhibitory factor in the developing brain. Fetal mouse brain cells can be changed from neuroepithelial cells to astrocytes in their developmental pathway by the exposure to BMP-2 as described previously.[16] It has been reported that Noggin is necessary to create neurons from neuroepithelial cells.[17] After spinal injury, neural stem cells differentiate into astrocytes, not into neurons. The up-regulation of BMP-2 or -7 after spinal injury may inhibit differentiation into neurons and promote that of astrocytes. In addition, stimulation by Noggin is thought to accelerate degeneration of neurons in spinal tissue after spinal injury.[18,19] However, the relationship between neurons and BMP-related molecules has not yet been fully established, particularly in the spinal cord. In the present study, BMP-2, BMPRs and Noggin were moderately stained in neurons in the spinal cord, indicating that BMP signaling might be related to spinal cord development.

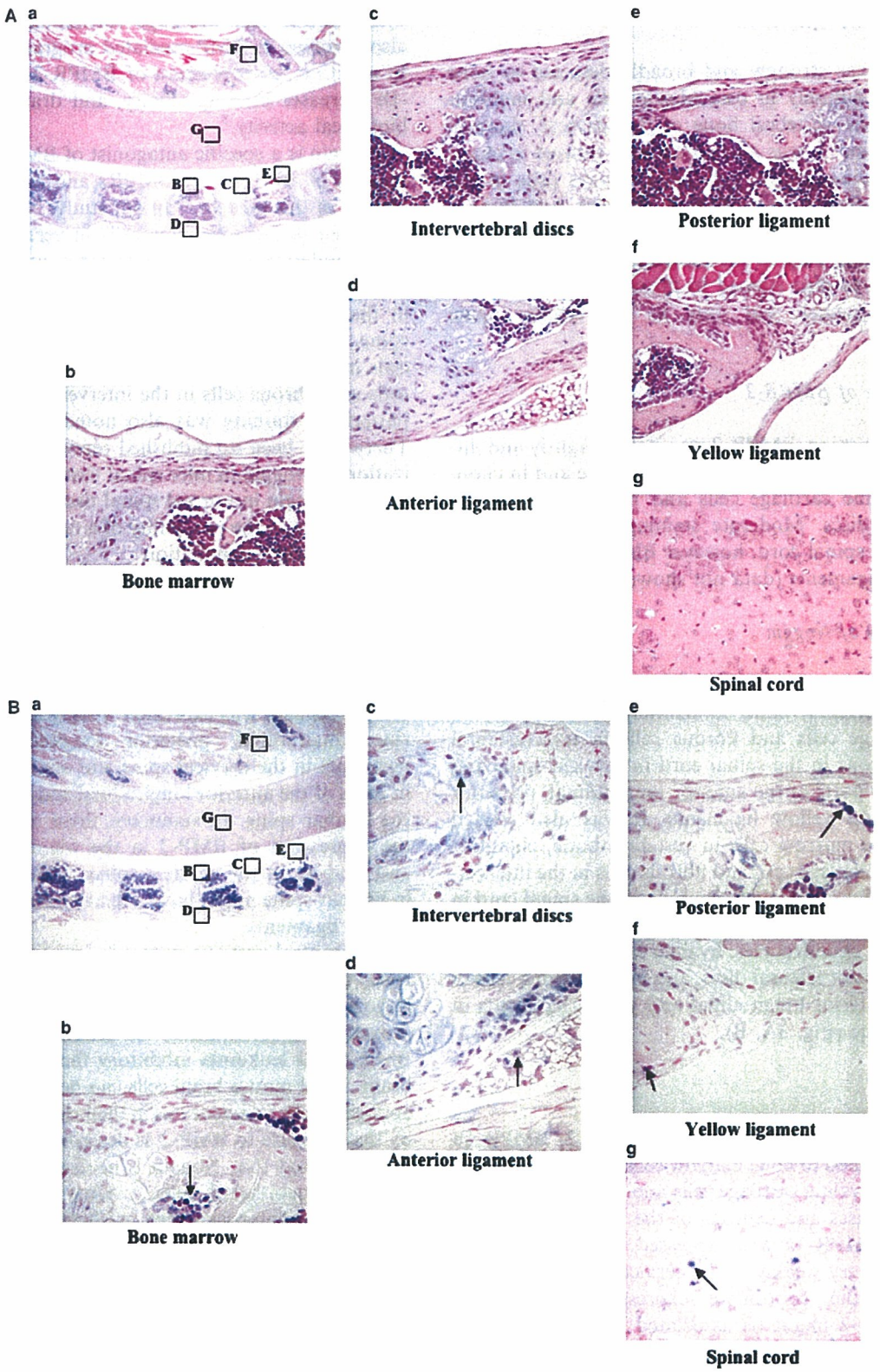

Fig. 3A. (a) Hematoxylin and eosin histochemistry of the cervical spine of the 3-week-old mouse corresponding to in situ hybridization of Noggin in Fig. 3B. (b) In situ hybridization of Noggin in the cervical spine of the 3-week-old mouse. In the whole cervical spine (a: original magnification: ×16), vertebral bone (b: original magnification: ×400), intervertebral discs (c: original magnification: ×400), anterior longitudinal ligament (d: original magnification: ×400), posterior longitudinal ligament (e: original magnification: ×400), yellow ligament (f: original magnification: ×400) and spinal cord (g: original magnification: ×400). Arrows in each figure point to strong staining of bone marrow cells (b), moderate staining of chondrocytes and hyaline cartilage cells (c), fibrous cells (d–f) and neurons (g).

Intervertebral discs act as 'shock absorbers' and joints during activity, allowing the spine to move freely. They consist of an outer fibrous ring and an inner nucleus pulposus. The discs are avascular, with sparsely distributed chondrocytes. It has been reported that BMPRs are present in cervical intervertebral discs in senescence-accelerated mice and in anterior margin cells in the cervical discs of a mouse spondylosis model.[11,12] In the current study, BMPR-1a was not stained in intervertebral discs, and BMP-2, BMPR-1b, -2, and Noggin were equally stained in chondrocytes, hyaline cartilage cells and fibrous cells in the cervical, thoracic and lumbar intervertebral discs. The relative distribution of BMP-2, BMPR-1b, -2 and Noggin in cervical, thoracic and lumbar intervertebral discs suggests that there is a relationship between their development and the BMP signaling pathway.

Bone marrow cells include pluripotent mesenchymal cells that are thought aid repair or maintain cells in other tissues, and produce various cytokines such as BMPs.[8] In this report, the expression of BMP-2, BMPR-1b, Noggin and particularly the strong expression of BMPR-1b in bone marrow cells, points to BMP signaling in bone marrow.

Recent studies have clearly demonstrated that BMP gene therapy with adenoviral vectors or rhBMP-2 implantation is useful for the induction of spinal arthrodesis or bone healing and regeneration in several animal models.[20] However, these studies have not provided sufficient data to warrant clinical application at this point.[21] There have been no reports using BMPRs or Noggin gene therapies in vivo in humans thus far. In this study, the expression of BMPR-1a or -1b in the yellow ligament, and Noggin in the anterior longitudinal, posterior longitudinal and yellow ligaments was detected by in situ hybridization. Understanding of the expression and action of these molecules may lead to the design of a gene therapy approach for the treatment of ligamentous ossification. However, further preclinical and clinical research and development are required before this technology will have direct clinical utility.

References

1. Miyazono K, Ichijo H, Heldin CH. Transforming growth factor-beta: latent forms, binding proteins and receptors. *Growth Factors* 1993;**8**:11–22.
2. Fujii M, Takeda K, Imamura T, et al. Roles of bone morphogenetic protein type I receptors and Smad proteins in osteoblast and chondroblast differentiation. *Mol Biol Cell* 1999;**10**:3801–13.
3. Ishidou Y, Kitajima I, Obama H, et al. Enhanced expression of type I receptors for bone morphogenetic proteins during bone formation. *J Bone Miner Res* 1995;**10**:1651–9.
4. Kaneko H, Arakawa T, Mano H, et al. Direct stimulation of osteoclastic bone resorption by bone morphogenetic protein (BMP)-2 and expression of BMP receptors in mature osteoclasts. *Bone* 2000;**27**:479–86.
5. Onishi T, Ishidou Y, Nagamine T, et al. Distinct and overlapping patterns of localization of bone morphogenetic protein (BMP) family members and a BMP type II receptor during fracture healing in rats. *Bone* 1998;**22**:605–12.
6. Gazzerro E, Gangji V, Canalis E. Bone morphogenetic proteins induce the expression of noggin, which limits their activity in cultured rat osteoblasts. *J Clin Invest* 1998;**102**:2106–14.
7. Holley SA, Neul JL, Attisano L, et al. The Xenopus dorsalizing factor noggin ventralizes Drosophila embryos by preventing DPP from activating its receptor. *Cell* 1996;**86**:607–17.
8. Shimakura Y, Yamazaki Y, Uchinuma E. Experimental study on bone formation potential of cryopreserved human bone marrow mesenchymal cell/hydroxyapatite complex in the presence of recombinant human bone morphogenetic protein-2. *J Craniofac Surg* 2003;**14**:108–16.
9. Zimmerman LB, De Jesus-Escobar JM, Harland RM. The Spemann organizer signal noggin binds and inactivates bone morphogenetic protein 4. *Cell* 1996;**86**:599–606.
10. Yonemori K, Imamura T, Ishidou Y, et al. Bone morphogenetic protein receptors and activin receptors are highly expressed in ossified ligament tissues of patients with ossification of the posterior longitudinal ligament. *Am J Pathol* 1997;**150**:1335–47.
11. Nakase T, Ariga K, Miyamoto S, et al. Distribution of genes for bone morphogenetic protein-4, -6, growth differentiation factor-5, and bone morphogenetic protein receptors in the process of experimental spondylosis in mice. *J Neurosurg* 2001;**94**(1 Suppl):68–75.
12. Takae R, Matsunaga S, Origuchi N, et al. Immunolocalization of bone morphogenetic protein and its receptors in degeneration of intervertebral disc. *Spine* 1999;**24**:1397–401.
13. Zhao M, Harris SE, Horn D, et al. Bone morphogenetic protein receptor signaling is necessary for normal murine postnatal bone formation. *J Cell Biol* 2002;**157**:1049–60.
14. Yoshimura Y, Nomura S, Kawasaki S, Tsutsumimoto T, Shimizu T, Takaoka K. Colocalization of noggin and bone morphogenetic protein-4 during fracture healing. *J Bone Miner Res* 2001;**16**:876–84.
15. Nakamura Y, Wakitani S, Nakayama J, Wakabayashi S, Horiuchi H, Takaoka K. Temporal and spatial expression profiles of BMP receptors and Noggin during BMP-2 induced ectopic bone formation. *J Bone Miner Res* 2003;**18**:1854–62.
16. Lein PJ, Beck HN, Chandrasekaran V, et al. Glia induce dendritic growth in cultured sympathetic neurons by modulating the balance between bone morphogenetic proteins (BMPs) and BMP antagonists. *J Neurosci* 2002;**22**:10377–87.
17. Lim DA, Tramontin AD, Trevejo JM, Herrera DG, Garcia-Verdugo A, Alvarez-Buylla A. Noggin antagonizes BMP signaling to create a niche for adult neurogenesis. *Neuron* 2000;**28**:713–26.
18. Gomes WA, Mehler MF, Kessler JA. Transgenic overexpression of BMP4 increases astroglial and decreases oligodendroglial lineage commitment. *Dev Biol* 2003;**255**:164–77.
19. Mekki-Dauriac S, Agius E, Kan P, Cochard P. Bone morphogenetic proteins negatively control oligodendrocyte precursor specification in the chick spinal cord. *Development* 2002;**129**:5117–30.
20. Nishida K, Kang JD, Gilbertson LG, et al. Modulation of the biologic activity of the rabbit intervertebral disc by gene therapy: an in vivo study of adenovirus-mediated transfer of the human transforming growth factor beta 1 encoding gene. *Spine* 1999;**24**:2419–25.
21. Takahashi J, Saito N, Ebara S, et al. Anterior thoracic spinal fusion in dogs by injection of recombinant human bone morphogenetic protein-2 and a synthetic polymer. *J Spinal Disord* 2003;**16**:137–43.

Volume 54(12): 1371–1378, 2006
Journal of Histochemistry & Cytochemistry
http://www.jhc.org

ARTICLE

Immunohistochemical Localization of α-Smooth Muscle Actin During Rat Molar Tooth Development

Akihiro Hosoya, Hiroaki Nakamura, Tadashi Ninomiya, Kunihiko Yoshiba, Nagako Yoshiba, Hiroyuki Nakaya, Shigeyuki Wakitani, Hirohito Yamada, Etsuo Kasahara, and Hidehiro Ozawa

Department of Oral Histology (AH,HNakamura), Institute for Dental Science (TN,HO), and Department of Endodontics and Operative Dentistry (HY,EK), Matsumoto Dental University, Shiojiri, Nagano, Japan; Division of Cariology, Department of Oral Health Science, Course for Oral Life Science, Niigata University Graduate School of Medical and Dental Sciences, Niigata, Japan (KY,NY); and Department of Orthopedic Surgery, Shinshu University Graduate School of Medicine, Matsumoto, Nagano, Japan (HNakaya,SW)

SUMMARY The dental follicle contains mesenchymal cells that differentiate into osteoblasts, cementoblasts, and fibroblasts. However, the characteristics of these mesenchymal cells are still unknown. α-Smooth muscle actin (α-SMA) is known to localize in stem cells and precursor cells of various tissues. In the present study, to characterize the undifferentiated cells in the dental follicle, immunohistochemical localization of α-SMA was examined during rat molar tooth development. Rat mandibles were collected at embryonic days (E) 15–20 and postnatal days (P) 7–28. Immunohistochemical stainings for α-SMA, periostin, Runt-related transcription factor-2 (Runx2), tissue nonspecific alkaline phosphatase (TNAP), and bone sialoprotein (BSP) were carried out using paraffin-embedded sections. α-SMA localization was hardly detected in the bud and cap stages. At the early bell stage, α-SMA-positive cells were visible in the dental follicle around the cervical loop. At the late bell to early root formation stage (P14), these cells were detected throughout the dental follicle, but they were confined to the apical root area at P28. Double immunostaining for α-SMA and periostin demonstrated that α-SMA-positive cells localized to the outer side of periostin-positive area. Runx2-positive cells were visible in the α-SMA-positive region. TNAP-positive cells in the dental follicle localized nearer to alveolar bone than Runx2-positive cells. BSP was detected in osteoblasts as well as in alveolar bone matrix. These results demonstrate that α-SMA-positive cells localize on the alveolar bone side of the dental follicle and may play a role in alveolar bone formation.
(J Histochem Cytochem 54:1371–1378, 2006)

KEY WORDS
α-smooth muscle actin
dental follicle
undifferentiated cell
rat molar
periostin

THE DENTAL FOLLICLE surrounding the tooth germ contains mesenchymal cells that are able to differentiate into osteoblasts, cementoblasts, and fibroblasts (Nanci 2003). As a result, this tissue is able to form the periodontal tissues including alveolar bone, cementum, and periodontal ligament. However, the characteristics and distribution of undifferentiated cells within the dental follicle and periodontal tissues are still unclear.

Previous reports have described α-smooth muscle actin (α-SMA) as a cytoskeletal protein that is localized to some stem and precursor cells (Cai et al. 2001; Kinner et al. 2002; Yamada et al. 2005). This protein has also been found in various tissues during tissue repair and regeneration following injury (Chaponnier and Gabbiani 2004; van Beurden et al. 2005). Thus, α-SMA may be a suitable marker of undifferentiated cells (Kinner et al. 2002). Additionally, in mature tissues, α-SMA is localized to pericytes of blood vessels, intestinal muscularis mucosae, and myoepithelial cells of mammary and salivary glands (Mukai et al. 1981; Skalli et al. 1986), which are required in a force-generating capacity. However, the temporospatial localization of α-SMA in developing and mature teeth has not been previously examined.

On the other hand, regeneration of periodontal tissues, lost as a result of periodontal disease, is a key

Correspondence to: Akihiro Hosoya, DDS, PhD, Department of Oral Histology, Matsumoto Dental University, 1780 Gobara Hirooka, Shiojiri, Nagano 399-0781, Japan. E-mail: hosoya@po.mdu.ac.jp

Received for publication March 29, 2006; accepted July 21, 2006 [DOI: 10.1369/jhc.6A6980.2006].

0022-1554/06/$3.30

objective of periodontal treatment. Several surgical techniques have been developed to assist with regeneration of periodontal tissues including guided tissue regeneration, bone grafting, and the use of enamel matrix derivative (Emdogain; Straumann, Basel, Switzerland), but their success is not predictable. Development of new periodontal regeneration therapies using the undifferentiated cells in the periodontal tissues thus remains ongoing. The human periodontal ligament contains multipotent stem cells that differentiate into osteoblasts, cementoblasts, and fibroblasts, and these cells could possibly be used to induce periodontal regeneration (Seo et al. 2004,2005). Additionally, the dental follicle has been utilized as a source of undifferentiated cells in in vitro and in vivo studies (Saito et al. 2005). Because the dental follicle and periodontal ligament are immunopositive for periostin (Kruzynska-Frejtag et al. 2004; Suzuki et al. 2004), this protein is often used as a marker of these tissues. However, determining the degree of cell differentiation could not be readily ascertained. A more definitive understanding of the periodontal tissue could assist with the development of regenerative methods using periodontal cells.

The differentiation process of alveolar bone-formative osteoblasts has also not been clarified. Bone morphogenetic proteins (BMPs) and/or transforming growth factor (TGF)-β act on undifferentiated cells and phosphorylate R-Smads through their receptors. These phosphorylated R-Smads subsequently interact with Smad4 and translocate to the nucleus (Derynck et al. 1998; Shi and Massague 2003). Thereafter, Runx2, the essential transcription factor for osteoblast differentiation, is expressed in osteogenic cells and induces the expression of bone matrix proteins such as osteopontin (OPN) and bone sialoprotein (BSP) (Lian et al. 2004). In these processes, expression of tissue nonspecific alkaline phosphatase (TNAP) is also increased (Hoshi et al. 1997; Hosoya et al. 2003).

In the present study, we show that α-SMA is specifically expressed in the dental follicle. In addition, to examine the distribution pattern of α-SMA and the differentiation process of these positive cells, immunohistochemical localization of α-SMA and other differentiation marker proteins were examined during rat molar tooth development. The marker of the dental follicle used was periostin-specific antibody. Observations of cell differentiation process in α-SMA-positive area were also undertaken and involved the use of Smad4-, Runx2-, OPN-, BSP-, and TNAP-specific antibodies.

Materials and Methods

All experiments were performed according to guidelines set forth by the Matsumoto Dental University Committee on Intramural Animal Use.

Western Blotting

First molar tooth germs of E15, 17, and 20 Wistar rats were removed from the mandible. Samples were dissolved in 100 μl of sample buffer containing 4% SDS, 20% glycerol, and 12% mercaptoethanol in 100 mM Tris–HCl (pH 6.8) and heated at 100C for 5 min. These lysates were quantified by BCA protein assay kit (Pierce Biotechnology; Rockford, IL), and an equal amount (30 μg) of each lysate was fractionated by SDS-PAGE using 12% polyacrylamide gel. Samples were then electrophoresed at 150 V for 60 min and transferred to a nitrocellulose membrane using 192 mM glycine and 20% methanol in 25 mM Tris–HCl (pH 8.3) at a constant amperage of 50 mA for 60 min. The membrane was immersed in 10 mM TBS, pH 7.4, containing 10% skim milk for 30 min to block nonspecific binding. It was subsequently incubated with mouse monoclonal antibody against human α-SMA (1A4;R&D Systems, Minneapolis, MN), diluted 1:1000 for 12 hr at 4C, and then with horseradish peroxidase (HRP)-conjugated anti-mouse IgG (Sigma; St Louis, MO) for 1 hr at room temperature. Immunoreactivity was visualized using ECL Western blotting detection reagents (Amersham Pharmacia Biotech UK Ltd.; Buckinghamshire, England) according to the manufacturer's instructions. The membrane was then reprobed in 2% SDS, 62.5 mM Tris–HCl (pH 6.7), and 100 mM 2-mercaptoethanol for 30 min at 50C and subsequently incubated with rabbit anti-mouse actin polyclonal antibody (Biomedical Technologies; Stoughton, MA), and HRP-conjugated anti-rabbit IgG (Sigma) for comparison of the amount of total protein.

Immunohistochemistry

Rat mandibles were collected at E15–20 and P7–28 and fixed with 4% paraformaldehyde in 0.1 M phosphate buffer (pH 7.4) for 24 hr at 4C. After demineralization with 10% EDTA, pH 7.4, for 3 weeks at 4C, the specimens were embedded in paraffin and sectioned at a thickness of 4 μm. Sections were then treated with 0.3% H_2O_2 in PBS, pH 7.4, for 30 min at room temperature to inactivate endogenous peroxidase. They were pretreated with 10% BSA (Seikagaku; Tokyo, Japan) in PBS for 1 hr at room temperature and incubated in mouse monoclonal antibodies against human α-SMA, human Smad4 (Santa Cruz Biotechnology; Santa Cruz, CA), and rabbit polyclonal antibodies against mouse Runx2 (Santa Cruz Biotechnology), rat TNAP (provided by Dr. Y. Ikehara), mouse OPN (provided by Dr. M. Fukae), human BSP (LF-120, provided by Dr. L.W. Fisher) for 12 hr at 4C. The antibodies against α-SMA, TNAP, OPN, and BSP were diluted to 1:500, and Smad4 and Runx2 antibodies were diluted to 1:100. Sections were reacted with Histofine Simple Stain rat MAX-PO (MULTI; Nichirei Co., Tokyo, Japan) for 1 hr at room temperature. Immune complexes were visualized using DAB (Envision kit; DAKO, Carpinteria, CA). Immunostained sections were then counterstained with hematoxylin. Non-immune mouse or rabbit sera were diluted to the same strength for use as negative controls. Control sections did not show any specific immunoreactivity.

Double-immunofluorescence staining was performed using mouse monoclonal antibody against human α-SMA and rabbit polyclonal antibody against human periostin (Bio-Vendor Laboratory; Heidelberg, Germany). Sections were pretreated with 10% BSA in PBS for 1 hr at room temperature

and incubated with 1:100 diluted primary antibodies for 12 hr at 4C. Sections were then incubated with 1:100 diluted Alexa-Fluor-488-conjugated anti-mouse IgG (Molecular Probes; Eugene, OR) and Alexa-Fluor-594-conjugated anti rabbit IgG (Molecular Probes) as secondary antibodies for 1 hr at room temperature. Samples were evaluated using a fluorescent microscope (Axioplan 2; Carl Zeiss, Jena, Germany) with the appropriate filter combinations.

Results

Localization of α-SMA During the Bud, Cap, and Early Bell Stages of Tooth Development

Western blotting analysis revealed that α-SMA antibody did not react with the lysate of E15 mandibular molar tooth germ. However, this antibody did react with the lysate of E17 and E20 tooth germs, with the intensity of reactivity increasing as tooth development progressed (Figure 1A).

Immunohistochemical localization of α-SMA was scarce in the tooth germ at the bud (E15) and cap (E17) stages (Figures 1B and 1C). At the early bell stage (E20), the dental follicle around the cervical loop displayed α-SMA immunoreactivity (Figures 1D and 1E). This immunoreactivity was seen within the cytoplasm of dental follicle cells possessing long cell processes (Figure 1F). The enamel organ and dental papillae showed no immunoreactivity.

Localization of α-SMA During the Late Bell and Root Formation Stages of Tooth Development

At the late bell stage (P7), α-SMA-positive cells were seen in the dental follicle surrounding the enamel organ

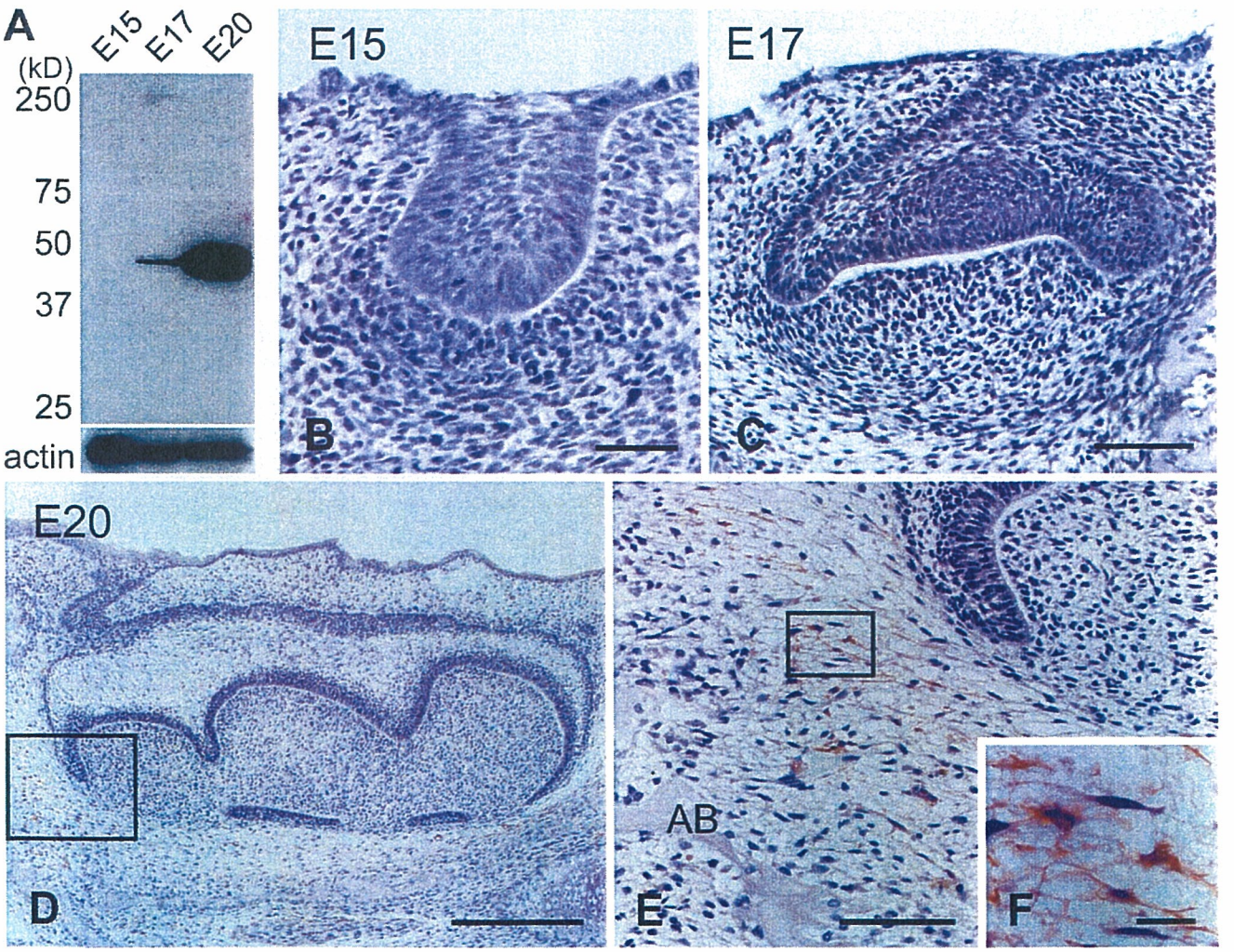

Figure 1 Western blotting analysis (**A**) and immunohistochemical staining of α-smooth muscle actin (αSMA) in the mandibular first molar at E15 (**B**), E17 (**C**), and E20 (**D–F**). Higher magnification of the boxed regions in **D** and **E** are shown in **E** and **F**, respectively. (**A**) α-SMA antibody reacted with cells in the E17 and E20 tooth germ. (**B,C**) α-SMA-positive cells are scarce in the tooth germs at the bud and cap stages. (**D,E**) The dental follicle cells around the cervical loop show α-SMA immunoreactivity at the early bell stage. (**F**) These cells exhibit long cell processes. AB, alveolar bone. Bars: **B,E** = 60 μm; **C** = 100 μm; **D** = 300 μm; **F** = 10 μm.

(Figure 2A). These cells seemed to localize on the alveolar bone side of the dental follicle (Figures 2B and 2C). Pericytes and smooth muscle cells of blood vessels surrounding the tooth germ and within the bone marrow displayed immunoreactivity. The surface of the alveolar bone, except the surface adjacent to the tooth germ, showed no immunoreactivity (Figure 2A). At the root formation stage (P14), intense immunostaining for α-SMA was observed in the dental follicle around Hertwig's epithelial root sheath (HRS). The dental follicle surrounding the enamel organ showed weaker immunoreactivity than that around HRS (Figures 2D–2F). As root formation progressed (P28), α-SMA-positive cells were confined to the apical region of the dental follicle (Figures 3A and 3C). In the upper region of the periodontal space, there was no immunoreactivity for α-SMA, except for that associated with the blood vessels (Figure 3B). In the pulp tissue, pericytes and smooth muscle cells of the blood vessels were positive for α-SMA, but odontoblasts and pulp cells showed no immunoreactivity (Figure 3A).

α-SMA and Periostin Localization in the Dental Follicle

In the root apex of P28, α-SMA-positive cells were localized to the dental follicle. Pericytes and smooth muscle cells of the blood vessels in the periodontal space were also immunopositive for α-SMA (Figure 4A). Periostin was localized to the apical region of the dental follicle and

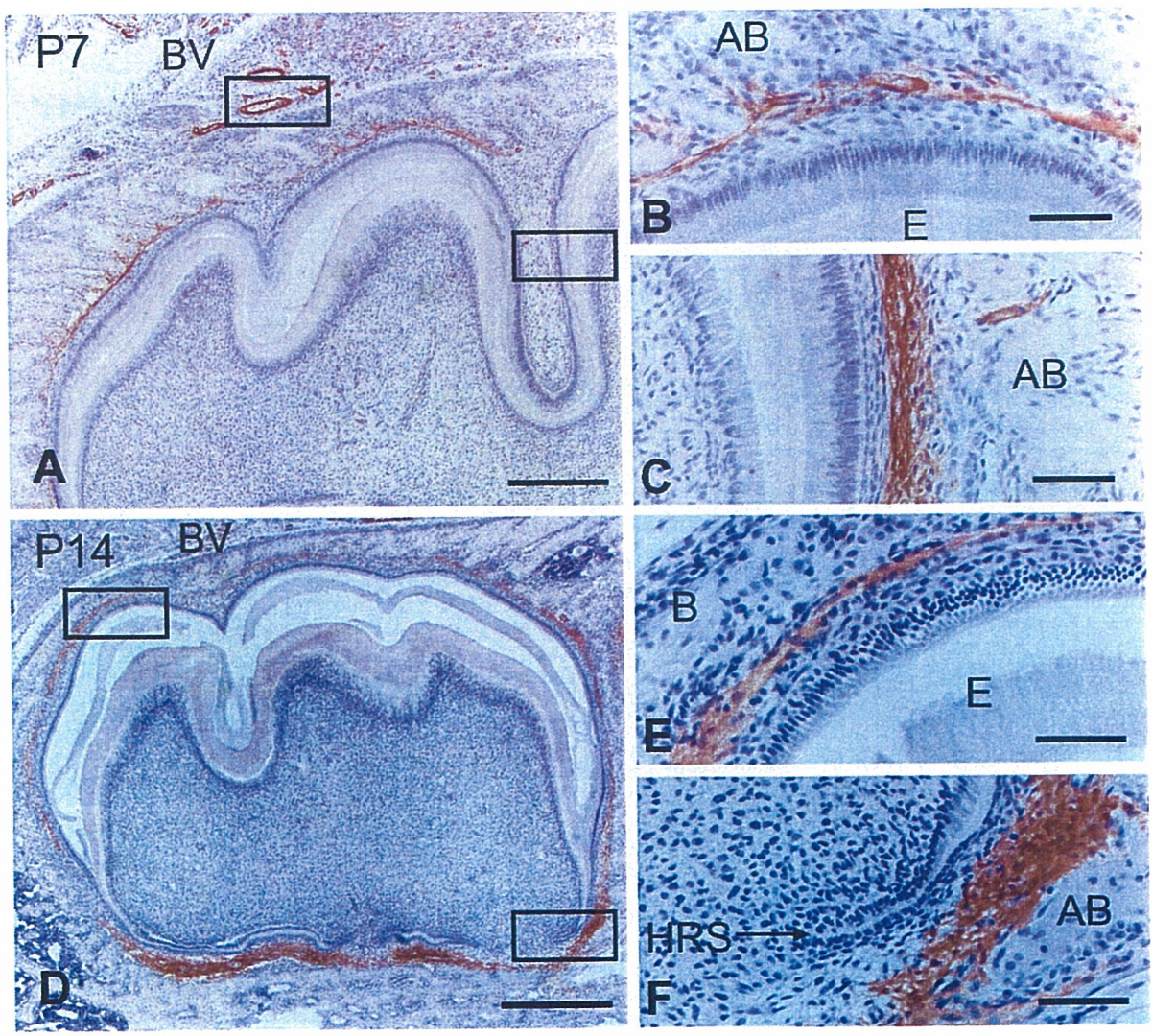

Figure 2 Immunohistochemical staining of α-SMA in the mandibular first molar at P7 (**A–C**) and P14 (**D–F**). Higher magnification of the boxed regions in **A** and **D** are shown in **B** and **C** and **E** and **F**, respectively. (**A**) α-SMA immunoreactivity is localized to the dental follicle surrounding the tooth crown at the late bell stage. (**B,C**) α-SMA-positive cells are visible on the alveolar bone (AB) side of the dental follicle. (**D–F**) Intense immunostaining for α-SMA is detected in the dental follicle along Hertwig's epithelial root sheath (HRS), whereas the dental follicle surrounding the tooth crown shows less immunoreactivity. BV, blood vessel; E, enamel. Bars: **A,D** = 600 μm; **B,C,E,F** = 100 μm.

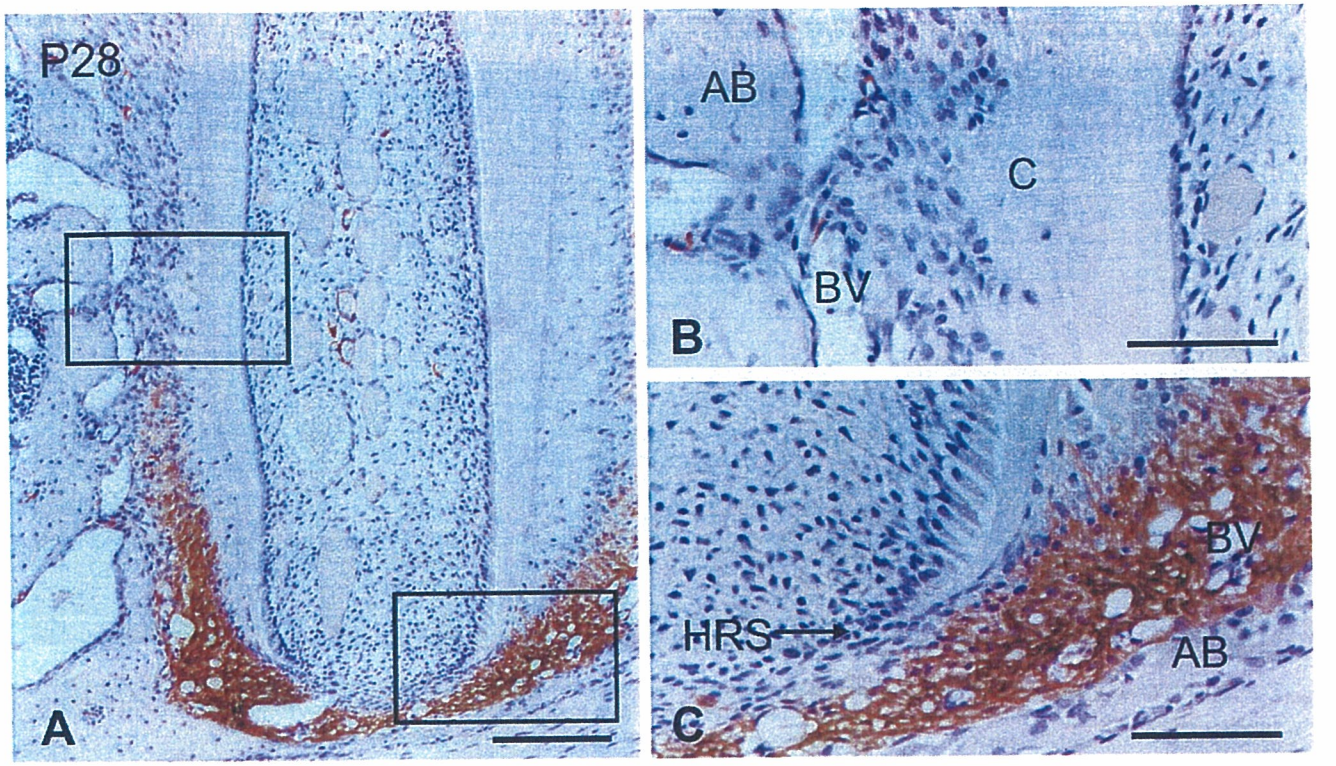

Figure 3 Immunohistochemical staining of α-SMA in the mandibular first molar at P28. Higher magnifications of the boxed regions in **A** are shown in **B** and **C**. **(A)** α-SMA immunoreactivity is apparent in the apical region dental follicle. **(B)** α-SMA immunoreactivity is not visible in osteoblasts, cementoblasts, and fibroblasts. **(C)** Intense immunostaining for α-SMA is seen in the dental follicle near HRS. AB, alveolar bone; BV, blood vessel; C, cementum. Bars: **A** = 150 μm; **B,C** = 40 μm.

to the periodontal ligament (Figure 4B). The merged image demonstrated that α-SMA-positive cells localized on the outer side of the dental follicle showing periostin immunoreactivity (Figure 4C). This staining pattern of α-SMA and periostin in whole regions of the dental follicle was consistent from E20 to P14 (not shown).

Distribution of Osteoblast Differentiation Marker Proteins in the Root Apex

In the root apex at P28, Smad4- and Runx2-positive cells were distributed in the apical dental follicle consistent with α-SMA-positive region (Figures 5A and 5B). TNAP-positive cells in the dental follicle localized closer to alveolar bone than Smad4- and Runx2-positive cells (Figure 5C). Immunostaining for OPN and BSP was detected in osteoblasts, as well as in alveolar bone matrix (Figures 5D and 5E).

Discussion

In the present study, α-SMA-positive cells were detected on the outer side of a periostin-positive area, and a relationship between α-SMA and periostin was observed during all stages of tooth development. Periostin is a protein specifically localized to the dental follicle and periodontal ligament (Kruzynska-Frejtag et al. 2004; Suzuki et al. 2004), suggesting that α-SMA-positive cells localize on the alveolar bone side of the dental follicle but not in the dental follicle near the outer enamel epithelium. This finding seems to confirm the idea that the dental follicle does not contain a homogeneous cell population and is divided into two regions (Schroeder 1991). In addition, because α-SMA-positive cells were localized on the alveolar bone side of the dental follicle, these cells are presumed to be involved in alveolar bone formation. This is supported by a previous study showing that MC3T3-E1, an osteoblast-like cell line, synthesizes α-SMA during the undifferentiated stage (Menard et al. 2000). Furthermore, because BMPs, especially BMP3, are expressed in some dental follicle cells, it is thought that BMPs regulate the formation of the osteoblast during root formation (Yamashiro et al. 2003). In the present study we determined the immunohistochemical localization of osteoblast differentiation marker proteins Smad4, Runx2, TNAP, OPN, and BSP, which are known to be downstream proteins of BMPs, in α-SMA-positive regions. Smad4- and/or Runx2-positive cells were detected in α-SMA-positive areas. In addition, TNAP-, OPN-, and BSP-positive cells were detected closer to the alveolar bone, suggesting that α-SMA-positive cells may differentiate into osteoblasts.

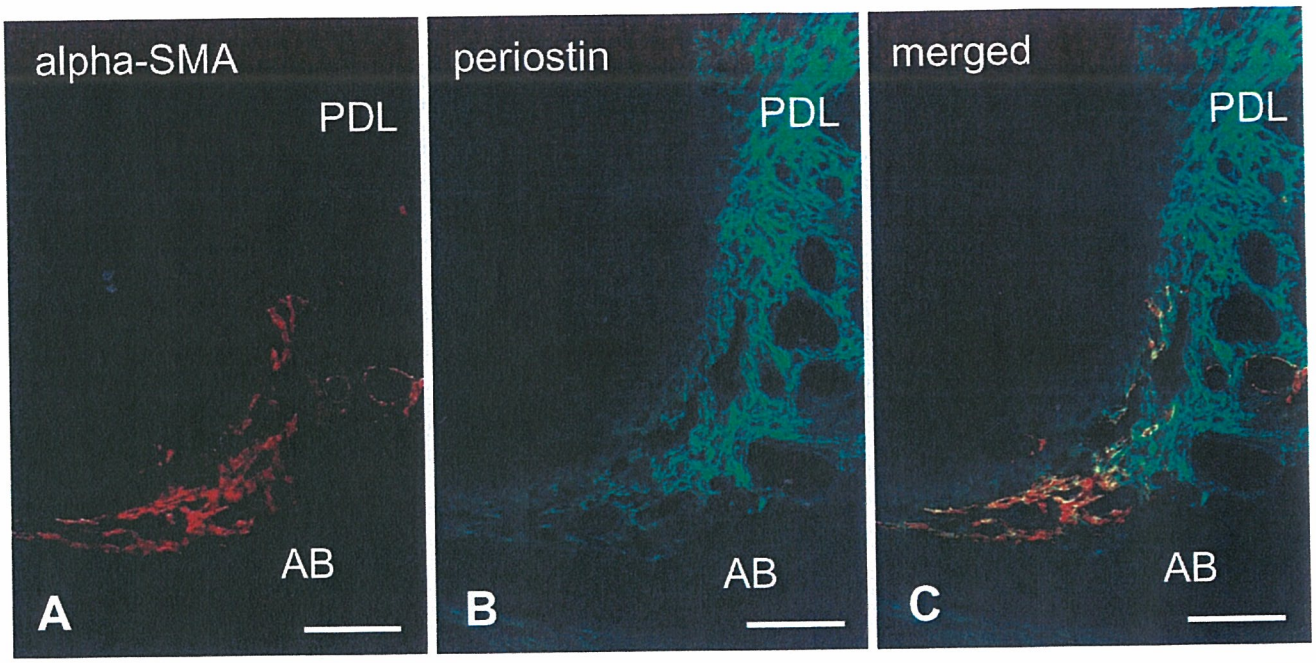

Figure 4 Double-immunofluorescence staining of α-SMA (shown in red) and periostin (in green) in the apical root at P28. **(A)** α-SMA localization is seen in the dental follicle at the root apex. **(B)** Periostin is localized to the dental follicle and periodontal ligament (PDL). **(C)** The area of α-SMA immunopositivity exists on the alveolar bone (AB) side of the periostin-positive area. Bar = 100 μm.

The areas of ectomesenchyme in bud (E15) and cap (E17) stages are believed to be undifferentiated. However, they were immunonegative for α-SMA. On the other hand, some dental follicle cells after early bell stage showed immunopositivity, suggesting that α-SMA begins to be expressed into some undifferentiated cells when they embark upon their differentiation process in the dental follicle. In addition, α-SMA-positive cells disappeared in the upper region of the periodontal tissues as root formation progressed (P28). Therefore, α-SMA may be a useful marker for determining the degree of cell differentiation in the dental follicle and in periodontal tissues.

The function of α-SMA is not clearly understood. α-SMA-expressing dental pulp cells increased with time in culture, and these cells have the contractile capacity to collagen–glycosaminoglycan analog of extracellular matrix in vitro (Brock et al. 2002). In addition, α-SMA is highly expressed in vascular smooth muscle cells, suggesting that it is required in a force-generating capacity. However, α-SMA null mice appear to have no abnormality in vascular contractility and blood pressure homeostasis, as a result of the partial substitution with other actin isoforms (Schildmeyer et al. 2000). It is thought that the dental follicle and periodontal ligament are implicated in the process of tooth eruption, and tooth eruption is linked to the contractility of fibroblasts. In the present study, α-SMA-positive region was shifted from the pericoronal dental follicle to the apical root at the beginning of root formation (P14) and confined to the apical root area by the late root formation stage (P28). Furthermore, although the number of α-SMA-positive cells decreased over time, the localization pattern in the apical root area was similar in 1-year-old rats (not shown). Therefore, expression of α-SMA may play a possible role in cell contractile capacity and tooth eruption. Meanwhile, α-SMA is also thought to act in the maintenance of the undifferentiated cell in an angiogenic capacity (Kinner et al. 2002; Hinz et al. 2003; Chaponnier and Gabbiani 2004). Further research into the role of α-SMA in tooth formation is required.

In conclusion, α-SMA is localized to the alveolar bone side of the dental follicle cells after the bell stage of tooth formation. This suggests that these cells might differentiate into osteoblasts and contribute to alveolar bone formation. Our results also suggest that α-SMA might be a useful marker of undifferentiated dental follicle cells for research into periodontal development and regeneration.

Acknowledgments

This work was supported by a Grant-in-Aid for Scientific Research from the Ministry of Education, Culture, Sports, Science and Technology of Japan.

The authors thank Dr. Y. Ikehara (Fukuoka University School of Medicine, Fukuoka, Japan), Dr. M. Fukae (Tsurumi University School of Dental Medicine, Yokohama, Japan), and Dr. L.W. Fisher (National Institute of Dental Research, National Institutes of Health, Bethesda, MD) for kindly providing the antibodies against TNAP, OPN, and BSP. We are also grateful to H. Komatsu (Matsumoto Dental University, Shiojiri, Japan) for technical support.

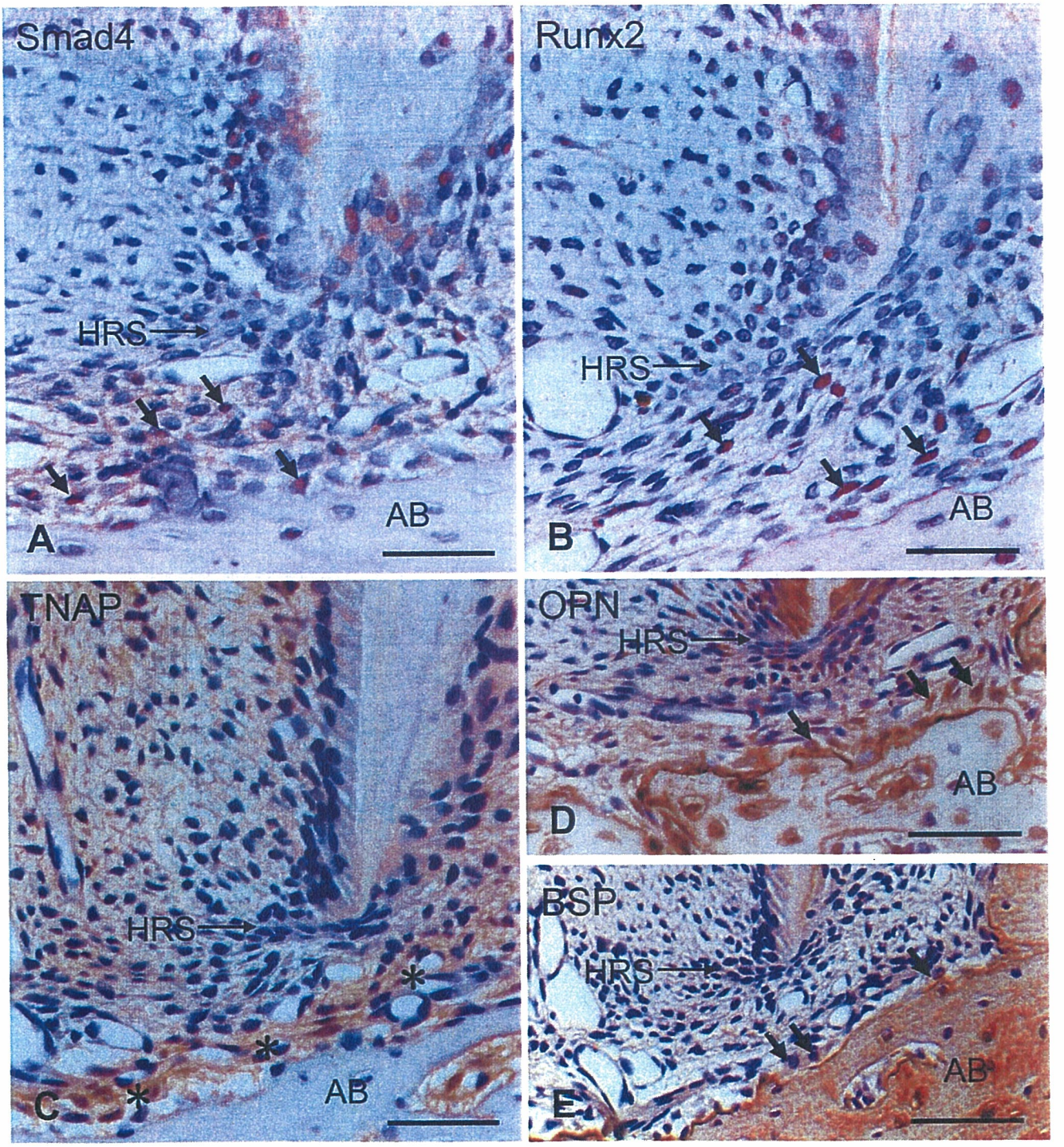

Figure 5 Immunohistochemical staining of Smad4 (**A**), Runx2 (**B**), tissue nonspecific alkaline phosphatase (TNAP) (**C**), osteopontin (OPN) (**D**), and bone sialoprotein (BSP) (**E**) in the apical root at P28. (**A,B**) Smad4- and Runx2-positive cells (arrows in **A,B**) are localized to the dental follicle at the root apex. (**C**) TNAP localization (asterisk) is detected at the periphery of the alveolar bone (AB). (**D,E**) OPN and BSP are localized to osteoblasts (arrows in **D,E**) and alveolar bone matrix. HRS, Hertwig's epithelial root sheath. Bar = 70 μm.

Literature Cited

Brock DP, Marty-Roix R, Spector M (2002) α-Smooth-muscle actin in and contraction of porcine dental pulp cells. J Dent Res 81: 203–208

Cai D, Marty-Roix R, Hsu HP, Spector M (2001) Lapine and canine bone marrow stromal cells contain smooth muscle actin and contract a collagen-glycosaminoglycan matrix. Tissue Eng 7:829–841

Chaponnier C, Gabbiani G (2004) Pathological situations characterized by altered actin isoform expression. J Pathol 204:386–395

Derynck R, Zhang Y, Feng XH (1998) Smads: transcriptional activators of TGF-beta responses. Cell 95:737–740

Hinz B, Dugina V, Ballestrem C, Wehrle-Haller B, Chaponnier C (2003) α-Smooth muscle actin is crucial for focal adhesion maturation in myofibroblasts. Mol Biol Cell 14:2508–2519

Hoshi K, Amizuka N, Oda K, Ikehara Y, Ozawa H (1997) Immunolocalization of tissue non-specific alkaline phosphatase in mice. Histochem Cell Biol 107:183–191

Hosoya A, Yoshiba K, Yoshiba N, Hoshi K, Iwaku M, Ozawa H (2003) An immunohistochemical study on hard tissue formation in a subcutaneously transplanted rat molar. Histochem Cell Biol 119:27–35

Kinner B, Zaleskas JM, Spector M (2002) Regulation of smooth muscle actin expression and contraction in adult human mesenchymal stem cells. Exp Cell Res 278:72–83

Kruzynska-Frejtag A, Wang J, Maeda M, Rogers R, Krug E, Hoffman S, Markwald RR, et al. (2004) Periostin is expressed within the developing teeth at the sites of epithelial-mesenchymal interaction. Dev Dyn 229:857–868

Lian JB, Javed A, Zaidi SK, Lengner C, Montecino M, van Wijnen AJ, Stein JL, et al. (2004) Regulatory controls for osteoblast growth and differentiation: role of Runx/Cbfa/AML factors. Crit Rev Eukaryot Gene Expr 14:1–48

Menard C, Mitchell S, Spector M (2000) Contractile behavior of smooth muscle actin-containing osteoblasts in collagen-GAG matrices in vitro: implant-related cell contraction. Biomaterials 21: 1867–1877

Mukai K, Schollmeyer JV, Rosai J (1981) Immunohistochemical localization of actin: applications in surgical pathology. Am J Surg Pathol 5:91–97

Nanci A (2003) Ten Cate's Oral Histology: Development, Structure, and Function. 6th ed. St. Louis, Mosby 240–274

Saito M, Handa K, Kiyono T, Hattori S, Yokoi T, Tsubakimoto T, Harada H, et al. (2005) Immortalization of cementoblast progenitor cells with Bmi-1 and TERT. J Bone Miner Res 20:50–57

Schildmeyer LA, Braun R, Taffet G, Debiasi M, Burns AE, Bradley A, Schwartz RJ (2000) Impaired vascular contractiliry and blood pressure homeostasis in the smooth muscle α-actin null mouse. FASEB J 14:2213–2220

Schroeder HE (1991) Oral Structural Biology. New York, Thieme Medical Publishers, 4–37

Seo BM, Miura M, Gronthos S, Bartold PM, Batouli S, Brahim J, Young M, et al. (2004) Investigation of multipotent postnatal stem cells from human periodontal ligament. Lancet 364:149–155

Seo BM, Miura M, Sonoyama W, Coppe C, Stanyon R, Shi S (2005) Recovery of stem cells from cryopreserved periodontal ligament. J Dent Res 84:907–912

Shi Y, Massague J (2003) Mechanisms of TGF-beta signaling from cell membrane to the nucleus. Cell 113:685–700

Skalli O, Ropraz P, Trzeciak A, Benzonana G, Gillessen D, Gabbiani G (1986) A monoclonal antibody against alpha-smooth muscle actin: a new probe for smooth muscle differentiation. J Cell Biol 103:2787–2796

Suzuki H, Amizuka N, Kii I, Kawano Y, Nozawa-Inoue K, Suzuki A, Yoshie H, et al. (2004) Immunohistochemical localization of periostin in tooth and its surrounding tissues in mouse mandibles during development. Anat Rec A Discov Mol Cell Evol Biol 281: 1264–1275

van Beurden HE, Von den Hoff JW, Torensma R, Maltha JC, Kuijpers-Jagtman AM (2005) Myofibroblasts in palatal wound healing: prospects for the reduction of wound contraction after cleft palate repair. J Dent Res 84:871–880

Yamada M, Kurihara H, Kinoshita K, Sakai T (2005) Temporal expression of alpha-smooth muscle actin and drebrin in septal interstitial cells during alveolar maturation. J Histochem Cytochem 53:735–744

Yamashiro T, Tummers M, Thesleff I (2003) Expression of bone morphogenetic proteins and Msx genes during root formation. J Dent Res 82:172–176

Materials Transactions, Vol. 46, No. 10 (2005) pp. 2260 to 2267

Improved Biocompatibility of Titanium–Zirconium (Ti–Zr) Alloy: Tissue Reaction and Sensitization to Ti–Zr Alloy Compared with Pure Ti and Zr in Rat Implantation Study

Yoshiaki Ikarashi[1], Kazuhiro Toyoda[2,*], Equo Kobayashi[3], Hisashi Doi[3], Takayuki Yoneyama[3], Hitoshi Hamanaka[3] and Toshie Tsuchiya[1]

[1]*Division of Medical Devices, National Institute of Health Sciences, Tokyo 158-8501, Japan*
[2]*Division of Pathology, National Institute of Health Sciences, Tokyo 158-8501, Japan*
[3]*Department of Metallurgy, Division of Biomaterials, Institute of Biomaterials and Bioengineering, Tokyo Dental and Medical University, Tokyo 101-0062, Japan*

Titanium–zirconium (Ti–Zr) binary alloy has better corrosion resistance and mechanical properties than commercially pure Ti. The present study was designed to determine the biocompatibility of Ti–Zr alloy by an implantation test in animal bodies in comparison with pure Ti, Zr, and chromium (Cr) implants as positive controls. Sample specimens were placed in a subcutaneous position in rats for 8 months. No significant decreases in body weight, the weight of any organ, or the weight of any organ relative to body weight were found in the implant groups compared to a no-implant control group. On hematological examination, small differences in several parameters were found in some groups, but these changes were not attributable to the materials implanted. Mitogen-induced blastogenesis was observed in similar degrees among all implant groups. These results suggest that the implantation of test samples did not cause systemic toxicity or a decrease in immune activity. The fibrous capsule membranes around the Ti and Ti–Zr alloy implants were thinner than those around Cr implants. The numbers of macrophages, inflammatory cells, and other cells involved in immune responses in and around the fibrous capsules of the Cr- and Ti-implant groups were higher than those of the Ti–Zr alloy- and Zr-implant groups. The Ti–Zr alloy had the lowest total score of tissue responses among the materials tested. None of the animals from the Ti-, Zr-, and Ti–Zr alloy-implant groups exhibited a skin reaction following exposure to Ti or Zr salt solutions. These results indicate the Ti–Zr alloy has better biocompatibility than Ti for use as an artificial surgical implant.

(Received April 28, 2005; Accepted August 31, 2005; Published October 15, 2005)

Keywords: *titanium alloy, titanium, biocompatibility, inflammation, hypersensitivity*

1. Introduction

Stainless steel and cobalt–chromium (Co–Cr) alloys have been widely used as materials in orthopedic and dental implants because of their biocompatibility, physical properties, and manufacturing ease.[1)] In general, these metallic alloys have excellent corrosion resistance and are not believed to cause any local or systemic responses. However, fretting corrosion of metallic implants is sometimes observed in contact with biological systems, causing the release of metallic ions from the implants.[2,3)] Elevated levels of metal ions have been found in blood, urine, and tissues of patients and animals that have received metal implants.[2–6)] Metallic ions, such as nickel (Ni), Co, and Cr, are known to cause adverse tissue reactions and allergy.[7–13)]

Titanium (Ti) and its alloys are currently considered the most attractive metallic materials for orthopedic and dental surgery. The use of Ti alloys is increasing due to their excellent mechanical strength, corrosion resistance, and good biocompatibility.[14–17)] These properties are attributable mainly to the formation of a stable titanium oxide (TiO_2) layer on the surface.[18,19)] However, the mechanical/tensile strength of commercially pure Ti is insufficient for its use as an artificial hip joint, pin, or screw,[20)] and its wear resistance is also inferior to that of stainless steels and Co–Cr alloys.[20)] The appearance of increased wear debris from Ti has been associated with inflammation, bone resorption, and pain.[18,19,21–24)] To improve mechanical strength and wear resistance, various elements have been added to create new Ti alloys. Ti–6Al–4V alloy is a high-strength Ti alloy, but its biocompatibility is considered lower than that of commercially pure Ti. The wear resistance and corrosion resistance of Ti–6Al–4V alloy are inferior to those of Ti, and Ti–6Al–4V alloy releases compounds and wear debris containing vanadium (V) or V ion, both of which are toxic.[18)] At present, it is difficult to avoid the wear and/or fretting of implanted alloys in a living body, resulting in the release of elements contained in the alloy and the formation of wear debris. Therefore, it is preferable not to use highly toxic elements in alloys.

Zirconium (Zr) belongs to the VIa group in the periodic table, as does Ti, and is known to have chemical properties similar to those of Ti.[20)] An insoluble oxide is formed on the surface in the air, and the surface oxide composition (zirconia) influences corrosion behavior. There is general agreement that Zr compounds have no local or systemic toxic effects.[25)] Based on this apparent lack of toxicity, Kobayashi *et al.* selected Zr as an alloying element to improve the properties of commercially pure Ti, and prepared a Ti–Zr binary alloy as a material for use in medical devices, such as artificial joints or bone plates.[20)] The hardness of Ti–50%(atom%) Zr alloy is 2.5 times as large as that of commercially pure Ti, suggesting the alloy's superior mechanical strength.[20)]

Besides mechanical properties, the biocompatibility of an alloy is important if it is to be used in implant devices. We previously observed that animals were sensitized to Cr by long-term implantation of corrosive Cr alloys.[26)] The animal model is a prevalent tool in examining tissue responses to implant material. The present study examined the biocom-

*Present address: Japan Tabacco Inc., Tokyo 130-8603, Japan